

---

# Ancient TL

www.ancienttl.org · ISSN: 2693-0935

---

Issue 23(1) - June 2005

<https://doi.org/10.26034/la.atl.v23.i1>

This issue is published under a Creative Commons Attribution 4.0 International (CC BY):

<https://creativecommons.org/licenses/by/4.0>



© Ancient TL, 2005

# Anomalous fading parameters and activation energies of feldspars

N.K. Meisl and D.J. Huntley

Department of Physics, Simon Fraser University, Burnaby, BC, V5A 1S6, Canada

(Received 9 February 2005; in final form 17 February 2005)

## Abstract

Anomalous fading parameters and activation energies are reported for a variety of feldspars and K-feldspars separated from sediments. While some interesting patterns emerge, prediction of the fading parameter from a measurement of the activation energy would appear to be unwise. There was a tendency for the activation energy to increase from 0.04 to 0.2 eV as the K content increases from 0 to 15 %.

## Introduction

Anomalous fading in feldspars is characterized by a decrease in the luminescence intensity measured during optical or thermal excitation as the delay time between irradiation and measurement increases. This decrease is not expected on the basis of measured thermal kinetic parameters and is, to a good approximation, linearly dependent on the logarithm of elapsed time since irradiation. Anomalous fading is now generally recognised as being due to the tunnelling of electrons from the ground state of the principal trap to nearby defects.

Quantitatively, anomalous fading is described by the fading parameter,  $g$ , which is the fractional decrease per decade, a decade here being a factor ten of time. Formally,

$$I = I_c(1 - g \log(t/t_c)) \quad (1)$$

where  $I$  is the intensity at time  $t$  and  $I_c$  is the intensity at an arbitrary time  $t_c$ . Thus  $g$  depends on the choice of  $t_c$ , though weakly.

The activation energy referred to here is a completely unrelated concept. In 1988, Hütt et al. made the observation that the luminescence intensity caused by 1.4 eV excitation increases with temperature. This increase is well described by the Arrhenius equation,

$$I = C \exp(-E/kT), \quad (2)$$

from which an activation energy,  $E$ , may be obtained for a sample. Despite several attempts to explain this effect, the underlying cause is as yet unknown.

There were two motivations for the present measurements. The first was that our measurements of anomalous fading make use of a control sample, referred to as a *témoin*, which should not fade, to correct for any changes in the instrument sensitivity and decay during luminescence measurements. The intensities of both the *témoin* and the sample increase with temperature. If the laboratory temperature changes from one measurement to another and the *témoin* and sample have different activation energies, then an error in the calculated fading parameter will occur unless this is corrected for. The effect can be quite significant. Since we have little control over our laboratory temperature we measured activation energies so that we can make the appropriate corrections. A better solution would be to control the laboratory temperature to 1 °C or less.

The second motivation was the possibility that the activation energy might be related in some unknown way to the tunnelling, and that there might be a relation between  $g$  and  $E$ . This possibility has been suggested by Poolton et al. (2003) who described some evidence for it. If such a relation existed then the lengthy measurements required to obtain  $g$  could be replaced by a simple measurement of  $E$ , an attractive proposition.

## Anomalous fading: experimental procedure

Measurements of the fading parameter  $g$  were as described in Huntley and Lamothe (2001), method 'b'. Aliquots were prepared by attaching thin slices of the minerals, or approximately 12 mg of K-feldspar grains separated from a sediment, to aluminium planchets using a Crystalbond<sup>1</sup>-acetone mixture and drying the planchet in the oven for one hour at 50 °C.

<sup>1</sup> Crystalbond 509: Aremco Products Inc., P.O. Box 517, 707-B Executive Blvd., Valley Cottage, N.Y. 10989, U.S.A.

Five aliquots of each sample were bleached if necessary, given a gamma dose of  $\sim 175$  Gy using a Nordion  $^{60}\text{Co}$  Gammacell<sup>2</sup>, heated at 120 °C for 16 hours, and measured using short shines at ca 2, 4, 8, 16, etc. days to about a year after irradiation. Excitation was 1.4 eV (IR) from LEDs and emission was measured using a Thorn-EMI 9635QB photomultiplier with Schott BG39 and Kopp 5-57 filters. This is designed to measure the violet emission band that is characteristic of K-feldspars. The témoin were K-feldspars separated from Tertiary sandstone from China Beach, Vancouver Island, British Columbia, sample CBSS.

#### Activation energy: experimental procedure

A detailed description of the equipment used for these measurements is given by Short (1993). Measurements were made using a conventional (Oxford style) thermoluminescence oven, over which was positioned an array of 1.4 eV (infrared) LEDs used to excite the sample. To avoid significant depletion of trapped charge, the LED array was pulsed. Emission from the sample passed through the centre of the diode array and was measured using a Thorn-EMI 9635QB photomultiplier tube with Schott BG-39 and Kopp 5-60 filters, similar to that in the first experiment.

For measurement, an aliquot previously used for the anomalous fading measurement was placed on the heating strip, using thermal compound to obtain a good thermal contact. Control for the experimental setup was automated by a PC running a program that controlled the power to the heating strip, pulsed the LED array and counted photons. Generally, one aliquot was measured per sample, however for samples for which individual aliquots yielded a range of fading parameters (specifically samples K12, #19 and #20), several aliquots were measured.

Aliquots were heated to 100 °C at a rate of 1 °C/s. Four LED pulses, two seconds in length each, exposed the sample at 20 °C, 40 °C, 60 °C and 80 °C. The temperature range and LED intensity were carefully chosen to ensure that sufficient emission could be measured while preventing substantial draining. Figure 1 is representative of the raw data obtained.

Note that the intensity increased with temperature and emission occurs at 20 °C, 40 °C, 60 °C and 80 °C, coinciding with the pulsing of the LEDs.

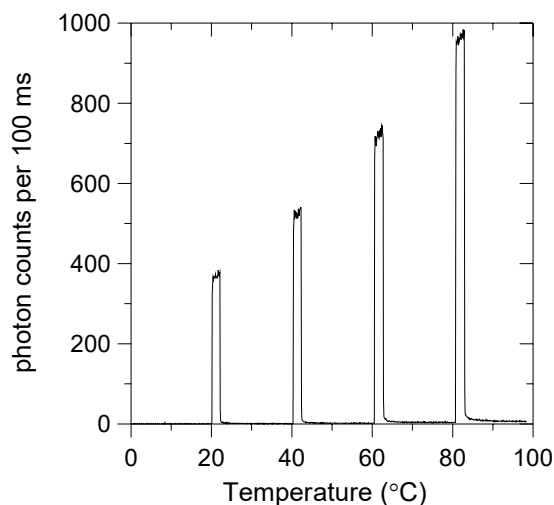


Figure 1: Photon emission vs. temperature for K8

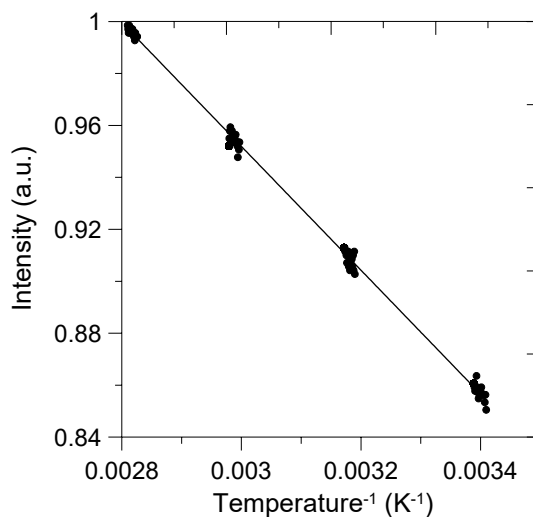


Figure 2: Fitted data used to extract  $E$  for K8

By fitting the data to the logarithm of equation 2,

$$\ln(I) = \ln(C) - E/kT, \quad (3)$$

$E$  was derived. A sample fit is shown in Figure 2.

In order to get an indication of how reproducible the method was, several different CBSS aliquots were measured over three days. Figure 3 shows the calculated  $E$  values, with error bars showing the uncertainty in fitting a straight line to the data with scatter. The x-axis shows the sequence in which the samples were measured.

<sup>2</sup> MDS Nordion, 447 March Road, Ottawa, ON K2K 1X8, Canada

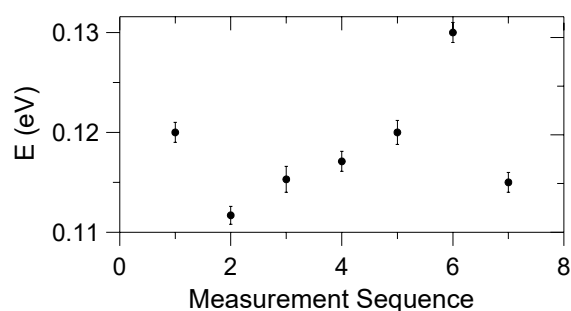


**Figure 3:** Measured  $E$  values for different CBSS aliquots

The least and greatest values measured for  $E$  differ by  $\sim 15\%$ . The first and last points in Figure 3 refer to the same aliquot, which was measured twice yielding  $E$  values that differ by less than 3%. The standard deviation of all the  $E$  values is 5%, presumably either due to grain variability or to a lack of perfect thermal contact, in addition to that derived from fitting the data.

To determine if  $E$  was dependent on either radiation dose or annealing temperature, two additional groups of CBSS samples were measured. Aliquots of one group were bleached and then given a variety of  $^{60}\text{Co}$  gamma cell radiation doses between 0 and 1500 Gy and then heated at 120 °C for 16 hours. The aliquots of the other group were heated at temperatures between 200 and 900 °C before radiation and heating. For both groups,  $E$  was found to be between 0.11 and 0.12 eV, thus there appears to be no dependence of the activation energy upon either radiation dose or annealing temperature.

### Results

The feldspar samples tested were alkali and plagioclase feldspars, and K-feldspar grains of a particular size-range isolated from sediments. Specific feldspar samples were obtained from Ward's Natural Science, the University of Adelaide and from various individuals. Natural sediment samples were obtained from a variety of locations. Care was taken to ensure that samples represented a wide range of fading parameters. The appendix lists  $g$  and  $E$  values, in addition to mineral content information where available, for the tested samples. Figure 4 shows graphs of fading parameter versus activation energy for a) alkali feldspars, b) plagioclase feldspars and c) K-feldspar grains separated from sediments. The error bars show the uncertainty in fitting data with scatter. In Figure 4c, different symbols have been used to distinguish between K-feldspar grains separated from Canadian prairie sediments and grains separated from other sediments.

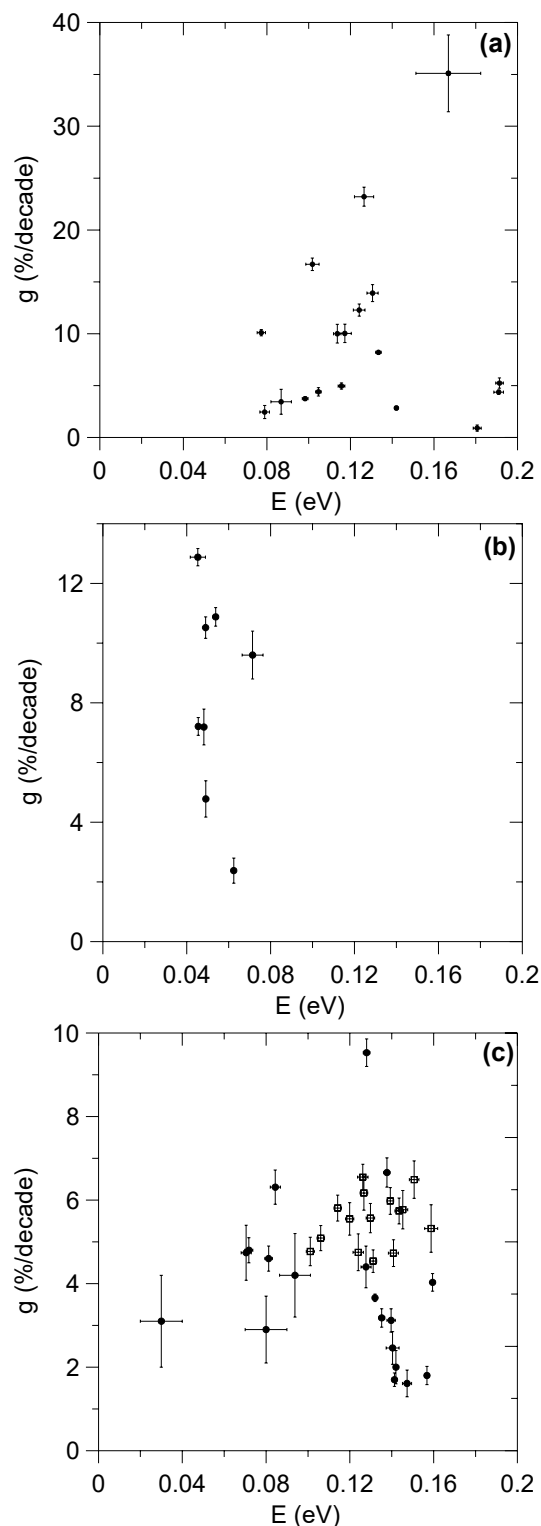


**Figure 4:** Fading parameter vs. activation energy for a) alkali feldspars, b) plagioclase feldspars and c) K-feldspar grains from sediment - open squares for Canadian prairie sediments, closed circles for other sediments

### Discussion

The range of measured  $E$  values was found to be 0.03 to 0.20 eV. This range is consistent with  $E$  values reported by others, e.g. Bailiff and Poolton (1991), Duller and Wintle (1991) and Short (2003). As Figure 4 demonstrates, it would not appear wise to predict the  $g$  of a sample from a measurement of its  $E$ . However, some interesting patterns were observed.  $E$  for plagioclases lies between 0.04 and 0.07 eV whereas for alkalis,  $E$  exhibits a much wider range between 0.08 and 0.2 eV. The pattern from K-feldspar grains separated from sediments is similar to that for alkali feldspar minerals, except that the fading parameters are much lower.

Two additional concerns about the  $E$  measurement procedure are worth noting. The first, reported by Short (2003), is that the determined  $E$  will depend on the emission band measured. The second, discussed by Baril and Huntley (2003), is that the excitation spectrum changes with increasing temperature. Specifically, they reported changes in the excitation spectrum with increasing temperatures (between 290 and 490 K) for orthoclase, albite and microcline samples and thus the activation energy is different for different excitation bands; what we measured here is an average over the LED emission band.

The data were also analyzed to determine if there was any relationship between  $E$  and the contents of several major elements in the sample: K, Na, and Ca. Figure 5 shows there appears to be a positive correlation between  $E$  and K content and negative correlations with Na and Ca contents.

### Conclusions

Activation energies were found for a collection of feldspars, both minerals and sediment extracts, for which fading parameters had been measured. Interesting patterns were observed, but determining the fading parameter of a sample from its activation energy would appear to be unwise. The activation energy is positively correlated to the K content and negatively correlated to Na and Ca contents.

### Acknowledgements

This research was financially supported by the Natural Sciences and Engineering Research Council of Canada.

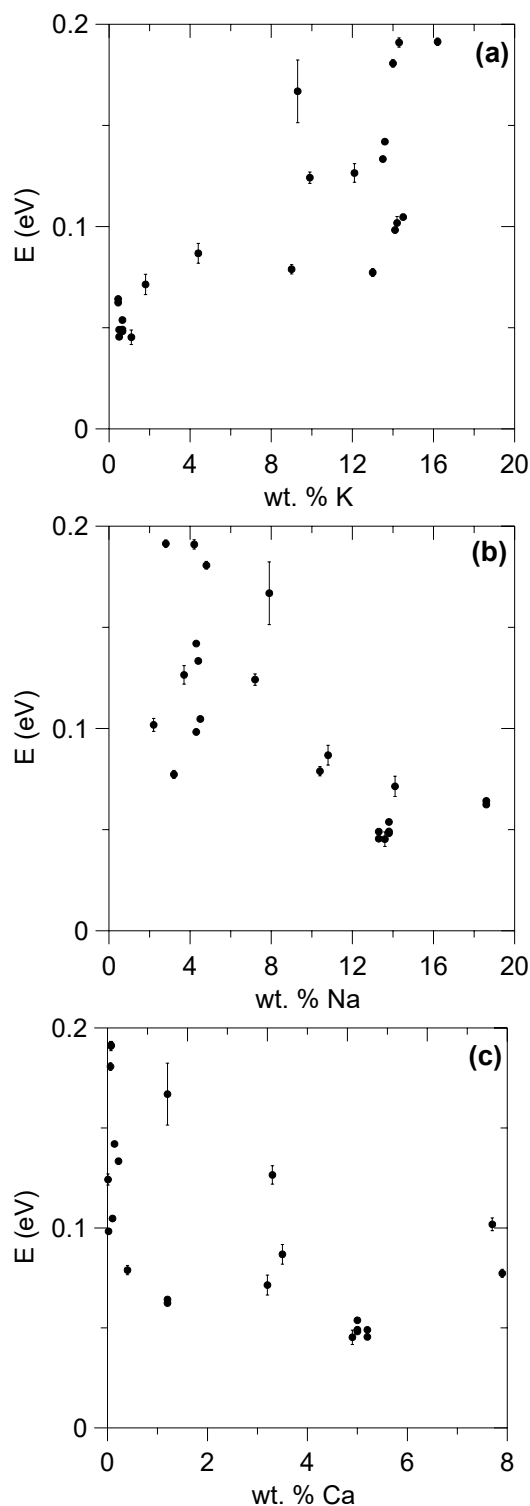


**Figure 5:** Activation energy variation with major element content: a) K, b) Na, c) Ca

## References

- Bailliff, I.K. and Poolton, N.R.J. (1991). Studies of charge transfer mechanisms in feldspars. *Nuclear Tracks and Radiation Measurements* **18**, 111-118.
- Baril, M.R. and Huntley, D.J. (2003). Infrared stimulated luminescence and phosphorescence spectra of irradiated feldspars. *Journal of Physics: Condensed Matter* **15**, 8029-8048.
- Duller, G.A.T. and Wintle, A.G. (1991). On infrared stimulated luminescence at elevated temperatures. *Nuclear Tracks and Radiation Measurements* **18**, 379-384.
- Huntley, D.J. and Lamothe, M. (2001). Ubiquity of anomalous fading in K-feldspars and the measurement and correction for it in optical dating. *Canadian Journal of Earth Sciences* **38**, 1093-1106.
- Huntley, D. J. and Lian, O. B. (in press). Some observations on tunnelling of trapped electrons in feldspars. *Quaternary Science Reviews*
- Hütt, G., Jaek, I. and Tchonka, J. (1988). Optical dating: K-feldspars optical response stimulation spectra. *Quaternary Science Reviews* **7**, 381-385.
- Poolton N.R.J, Malins A.E.R, Quinn F.M., Pantos, E., Andersen, C.E., Bøtter-Jensen, L., Johnsen, O. and Murray, A.S.. (2003). Luminescence excitation characteristics of Ca-, Na- and K-aluminosilicates (feldspars), in the stimulation range 20-500 eV: optical detection of XAS. *Journal of Physics D: Applied Physics* **36**, 1107-1114.
- Short, M.A. (1993). *Some aspects of optically stimulated luminescence for sediment dating*. M.Phil. thesis University of Hong Kong, 2.1-2.26.
- Short, M.A. (2003). *An investigation into the physics of infrared excited luminescence of irradiated feldspars*. PhD. Thesis, Simon Fraser University. 64-75.

**Reviewer**  
Ian Bailiff

## Appendix: Activation energies, fading parameters and major element contents in wt. %

The feldspars are a subset of those for which fading parameters are given in Huntley and Lamothe (2001) and Huntley and Lian (in press); a fading parameter listed here is for a single aliquot and may differ from that published, which is usually an average for 5 aliquots. Values of 'g' are for  $t_c = 2$  days after irradiation. Feldspars are from Canada unless otherwise stated. Of the 32 sediments, 22 are from Canada and the remainder are from New Zealand, the USA and Scandinavia. The three K12 results are for different crystals. The three #19 results are for slices from the same crystal; the analyses were done on a different portion of the same sample, similarly for the two #20 results.

**Alkali feldspars, listed in order of decreasing K content**

Sample	E (eV)	g (%/decade)	K	Na	Ca	Fe	Mg	Others > 0.01	
K13	0.191 ± 0.002	5.2 ± 0.5	16.2	2.8	0.07	0.07	0.03		microcline, Madawaska, Ontario. Ward's 46E 5124
HFC	0.105 ± 0.001	4.4 ± 0.4	14.5	4.5	0.10	0.08	0.01		perthite, Ontario
K10	0.191 ± 0.002	4.4 ± 0.2	14.3	4.2	0.07	0.04	n.d.		microcline, Keystone, S. Dakota, U.S.A Ward's #1 of 45 E 2941
K9	0.098 ± 0.001	3.7 ± 0.2	14.1	4.3	0.02	0.06	n.d.	0.04 P	microcline, var. amazonite, Kola peninsula, Murmansk, Russian Federation, Ward's #5 of 45 E 2941 & 46E 5164
K6	0.181 ± 0.002	0.9 ± 0.3	14.0	4.8	0.06	0.1	0.01	0.24 P	microcline, Ward's 45W 9252
K8	0.142 ± 0.001	2.8 ± 0.2	13.6	4.3	0.14	0.19	0.03		perthite (microcline & albite), Perth, Ontario, Ward's #4 of 45 E 2941 & 46E 0514
K3	0.133 ± 0.001	8.2 ± 0.2	13.5	4.4	0.22	0.08	n.d.	0.07 Ba	orthoclase, Red Lodge, Montana, U.S.A., U.B.C. TC313A6

K11	0.127 ± 0.005	23.4 ± 0.9	12.1	3.7	3.3	0.77	0.33	0.10 Ti, 0.18 Ba, 0.02 P, 0.03 Mn	orthoclase (Carlsbad Twin). Gothic, Colorado, U.S.A., Ward's #3 of 45 E 2941
K7	0.124 ± 0.003	12.2 ± 0.6	9.9	7.2	0.01	0.24	0.01		microcline, Crystal Peak, Colorado, U.S.A Ward's #2 of 45E 2941
PLTF	0.167 ± 0.016	35.1 ± 3.7	9.3	7.9	1.2	0.59	0.21	0.11 Ti, 0.14 Ba, 0.05 P, 0.02 Mn	Puy de la Tache, France
A5	0.079 ± 0.002	2.5 ± 0.6	9.0	10.4	0.40	0.26	0.05	0.03 Ba	"albite", Bancroft, Ontario, Ward's #7 of 45 E 2941
A4	0.087 ± 0.005	3.4 ± 1.2	4.4	10.8	3.5	3.3	1.65	0.74 Ti, 0.05 Ba, 0.30 P, 0.10 Mn	anorthoclase, Larvik, Norway, Ward's #6 of 45 E 2941
K12	0.116 ± 0.002	5.0 ± 0.3	-	-	-	-	-		orthoclase, India, Ward's 49E 5919
K12	0.131 ± 0.003	13.9 ± 0.8	-	-	-	-	-		orthoclase, India, Ward's 49E 5919
K12	0.117 ± 0.003	10.0 ± 0.9	-	-	-	-	-		orthoclase, India, Ward's 49 <sup>E</sup> 5919

**Plagioclase feldspars, listed in order of increasing Ca content**

Sample	E (eV)	g (%/decade)	K	Na	Ca	Fe	Mg	Others > 0.01	
P18	0.062 ± 0.001	2.4 ± 0.4	0.45	18.6	1.2	0.01	n.d.	0.05 Ba	oligoclase, Virginia, U.S.A.
#17	0.071 ± 0.005	9.6 ± 0.8	1.8	14.1	3.2	0.61	0.2	0.03 Ti	oligoclase, Arendal, Norway
#18	0.045 ± 0.004	12.9 ± 0.3	1.1	13.6	4.9	0.19	0.02		oligoclase, Sweden
#19	0.054 ± 0.001	10.9 ± 0.3	0.66	13.8	5	0.05	0.03		oligoclase, Renfrew County,
#19	0.048 ± 0.001	7.2 ± 0.6	"	"	"	"	"		"
#19	0.049 ± 0.001	4.8 ± 0.1	"	"	"	"	"		"
#20	0.046 ± 0.001	7.2 ± 0.3	0.5	13.3	5.2	0.15	0.01		oligoclase, Mitchell County, N. Carolina, U.S.A.
#20	0.049 ± 0.001	10.5 ± 0.4	"	"	"	"	"		"

**Other minerals**

Sample	E (eV)	g (%/decade)	K	Na	Ca	Fe	Mg	Others > 0.01	
BRS	0.102 ± 0.003	16.7 ± 0.6	14.2	2.2	7.7	0.29	0.09	0.04 Ti, 0.30 Ba, 0.02 Mn	sanidine Kettle Valley, B.C., contains fluorite
WCRS	0.077 ± 0.002	10.1 ± 0.3	13	3.2	7.9	0.37	0.12	0.04 Ti, 0.30 Ba, 0.03 Mn	sanidine, Kettle Valley, B.C. , contains fluorite
MCG	0.053 ± 0.007	1.0 ± 0.4	-	-	-	-	-		granodiorite, McKay Cr., North Vancouver, B.C.
CCF	0.1137 ± 0.002	10.0 ± 0.9	-	-	-	-	-		

**K-feldspar separated from sediments****Canadian prairie sediments**

Sample	E (eV)	g (%/decade)
SAW01-07	0.127 ± 0.002	6.2 ± 0.4
SAW01-20	0.139 ± 0.002	6.0 ± 0.3
SAW01-21	0.144 ± 0.002	5.7 ± 0.3
SAW01-22	0.145 ± 0.002	5.8 ± 0.5
SAW01-25	0.151 ± 0.002	6.5 ± 0.5
SAW01-27	0.126 ± 0.003	6.6 ± 0.3
SAW01-28	0.159 ± 0.003	5.3 ± 0.6
SAW02-01	0.120 ± 0.002	5.6 ± 0.4
SAW02-04	0.101 ± 0.002	4.8 ± 0.3
SAW02-06	0.124 ± 0.003	4.8 ± 0.4
SAW02-10	0.131 ± 0.002	4.5 ± 0.3
SAW02-13	0.141 ± 0.002	4.7 ± 0.3
SAW02-14	0.130 ± 0.002	5.6 ± 0.4
SAW02-15	0.114 ± 0.002	5.8 ± 0.3
SAW03-02	0.071 ± 0.002	4.7 ± 0.7
SAW97-12	0.106 ± 0.002	5.1 ± 0.3

**Other sediments**

From Canada (1-6), the U.S.A. (7-8), Scandinavia (9-10) and New Zealand (11-16)

	Sample	E (eV)	g (%/decade)
1	CCLI	0.072 ± 0.002	4.8 ± 0.3
2	BLRL2	0.081 ± 0.002	4.6 ± 0.3
3	TML1	0.132 ± 0.001	3.7 ± 0.1
4	TAG11	0.140 ± 0.003	2.5 ± 0.4
5	SAW94-62	0.084 ± 0.002	6.3 ± 0.4
6	BUCT	0.138 ± 0.002	6.7 ± 0.4
7	SN45	0.135 ± 0.001	3.2 ± 0.2
8	GP10	0.160 ± 0.001	4.0 ± 0.2
9	HJN4	0.142 ± 0.001	2.0 ± 0.4
10	HJR4	0.157 ± 0.001	1.8 ± 0.2
11	CKDS	0.140 ± 0.002	3.1 ± 0.3
12	RHIS	0.141 ± 0.001	1.7 ± 0.2
13	OTP10	0.128 ± 0.002	4.4 ± 0.5
14	PR11	0.030 ± 0.010	3.1 ± 1.1
15	GBDS4	0.080 ± 0.010	2.9 ± 0.8
16	HBTSI	0.094 ± 0.007	4.2 ± 1.0



# Revisiting TL: Dose measurement beyond the OSL range using SAR

M. Jain<sup>1\*</sup>, L. Bøtter-Jensen<sup>1</sup>, A.S. Murray<sup>2</sup>, P.M. Denby<sup>1</sup>,  
S. Tsukamoto<sup>3</sup> and M.R. Gibling<sup>4</sup>

<sup>1</sup> Risø National Laboratory, DK-4000 Roskilde, Denmark.  
(\* Corresponding author [mayank.jain@risoe.dk](mailto:mayank.jain@risoe.dk))

<sup>2</sup> Nordic Laboratory for Luminescence Dating, Department of Earth Sciences, Århus University, Risø National Laboratory, DK-4000 Roskilde, Denmark

<sup>3</sup> Department of Geography, Tokyo Metropolitan University, Hachioji, Tokyo 192-0397, Japan

<sup>4</sup> Department of Earth Sciences, Dalhousie University, Halifax, Nova Scotia, B3H 3J5, Canada

(Received 3 May 2005; in final form 25 May 2005)

## Abstract

We show here that isothermal TL (ITL) at 310 and 320°C can be used to extend the luminescence dating range in quartz. These signals have markedly different behaviour than the OSL signal with respect to dose response and bleaching efficiency using blue light; this suggests that the 325°C TL peak, from which these signals are likely to be derived, perhaps, consists of traps with very different optical depths and saturation characteristics.

The feldspar IRSL signal (blue emission) shows significant dose under-estimation on account of fading. This problem is partly circumvented by measurements using blue ITL at 310°C. The red ITL signal at 310°C does not show dose underestimates. A firm conclusion as to whether this signal fades or not can, however, only be made with a better understanding of sensitivity changes during the red ITL measurement of the natural signal. Both blue and red ITL signals in feldspars perhaps use the same trap. The fading and/or sensitivity changes, therefore, relate to the recombination centre.

On account of the high dose at which saturation appears, the ITL signal from quartz at 310 and 320°C is the best candidate for extending the dose range up to 1.4 kGy in samples from the southern Indo-Gangetic plains.

## Keywords

*Isothermal TL, Red emission, Quartz, Feldspars, Fading, Indo-Gangetic plains*

## Introduction

Over the last decade optically stimulated luminescence (OSL) dating of quartz has been established as a robust sediment dating method (Murray and Olley, 2002). This method relies on measurement of a light sensitive signal generally referred to as the fast OSL component. Unfortunately an early saturation of the signal responsible for the fast component limits the OSL dating range using quartz. Nevertheless, because of the greater likelihood that this signal was zeroed during sediment transport, under either sub-aerial and sub-aqueous conditions, the OSL signal is more likely to provide an accurate sedimentation age than the thermoluminescence (TL) signal.

In our experience many samples from the Indian subcontinent give a quartz OSL signal which saturates at about 100 - 150 Gy. Combined with dose rates of ~ 3 - 5 Gy/ka, this gives an OSL dating limit of about 20 - 50 ka. This dating limit greatly restricts investigations of the climate and tectonic changes that have shaped the Indian sub-continent during the Late Quaternary. A good example is the difficulty in dating the large sediment pile in the Himalayan foreland basin, commonly referred to as the Indo-Gangetic plains. This constitutes an excellent archive of the influence of climate, tectonism and sea level changes on one of the worlds largest and most dynamic river systems, but this archive cannot be interpreted without a chronological framework.

One way of breaking this age barrier is to explore quartz signals other than the fast OSL component. Alternatively, one can make use of luminescence signals from feldspar if due allowance for signal fading is made (Huntley and Lamothe, 2001). An important aspect of any new approach should be the ability to measure dose using a single small sub-sample (aliquot) so that by making several such measurements one can obtain a precise estimate of equivalent dose as well as an assessment of bleaching. Previously reported approaches to extending the age range include:

*(i) Quartz*

The slowly decaying OSL signal in quartz saturates above 1 kGy (Singarayer and Bailey, 2003). However, the rate of decay when stimulated using blue light (470Δ30 nm) is very low; this causes a poor signal-to-noise ratio. Also rather long times (several ks) are required to empty the luminescence signal during the measurement. Owing to these constraints a routine dating method using the slow OSL component is not yet practical.

Two important quartz TL dating signals, from the so called 325 and 375°C peaks, have been identified (Aitken 1985). Previous attempts to use the 325°C peak have been based on a comparison of bleached and unbleached TL peaks (e.g. Franklin and Hornyak, 1990). It has been shown earlier that dose-response curves using the 325°C TL signal have a significantly higher saturation level than the OSL signal (Figure 6a in Jain et al., 2005); in these samples from the Thar Desert the apparent dose saturation levels in multiple-aliquot growth curves were about 200 Gy for the OSL signal and about 450 Gy for the 325°C TL signal. There are also examples of measured quartz TL doses of up to 400 Gy from the coastal dune succession of southeast Australia (Huntley and Prescott, 2001). In general, however, a large scatter in the multiple aliquot data renders it difficult to make a direct, meaningful comparison of the TL and OSL saturation characteristics. In fact the differences in the dose saturation levels are generally hidden under the scatter in the data. Regarding the 375°C TL peak, Murray and Wintle (2000a) developed a single-aliquot regenerative-dose method using the isothermal TL (ITL) signal at 340°C. There was, however, only a limited improvement in the saturation level compared to the OSL and the residual levels in modern samples were high.

A completely different TL signal with emission in the 600-640 nm band can potentially extend the age range as it has very high saturation levels (> 20 kGy). However, this signal is strongest in volcanic quartz

(Fattahi and Stokes, 2000), and generally weak in quartz of plutonic origin.

*ii) Feldspars*

The dose saturation level in feldspars is generally acknowledged to be greater than that in quartz (e.g. Wallinga et al., 2001). However, because of the signal fading demonstrated in many samples (Huntley and Lamothe, 2001) the accuracy of feldspar ages is very dependent on how well one can correct for the age underestimation. These fading corrections are either model dependent or based on independent age control. In order to tackle fading, different emission signals from feldspars have been examined. For example, it has been suggested that the red emission from feldspars shows little or no fading (Zink and Visocekas, 1997; Fattahi and Stokes, 2003).

In general there have been few systematic investigations into the use of the TL signal using a single aliquot method (for example, Murray and Wintle, 2000a). An important reason for this is a shift in thrust to OSL dating in the last decade or so. Although, it is well known that TL is not as sensitive to daylight as the fast OSL signal, TL can potentially be used for dating old samples where burial doses are likely to be much greater than any residual doses. If dose saturation levels are high (>500 Gy) then these TL signals can potentially be used for dating beyond the OSL age range. In this contribution we test the use of ITL signals on single aliquots of quartz and feldspars for extending the age range. In particular, we present new results on the UV ITL emission from quartz and red ITL emission from feldspar.

**Experimental details**

Samples reported in this study were collected from exposed river sections in the southern Indo-Gangetic plains (Gibling et al., 2005). The main sediment sources are from the Himalayas. However, southern cratonic contributions are also significant. Thus one expects a mixture of granitic and metamorphosed quartz and feldspars in these samples.

Coarse grains of quartz (60 – 105 μm) were extracted from various sediment samples by routine treatment employing 10% hydrochloric acid (HCl) followed by sieving and 60 minutes of hydrofluoric acid (HF). The purity of the quartz extracts was confirmed using IR stimulation after a regeneration dose. The mixed sample from immediately prior to the HF treatment was considered as a feldspar sample. Although this mixture consists of quartz and feldspars, it can be effectively considered to give only feldspar luminescence signal; this is because there was no detectable signal from pure quartz aliquots in both

IRSL and red isothermal TL, and in the blue isothermal TL the quartz signal comprised <0.5% of the signal from the quartz and feldspar mixture. No attempt was made to separate various feldspar minerals. The results reported here are, therefore, based on mixed feldspar mineralogy.

An automated Risø TL/OSL reader (TL/OSL-DA-15) (Bøtter-Jensen et al., 2002) was used for all measurements. Blue light stimulation used an array of 28 LEDs (470Δ30 nm) delivering ~50 mW.cm<sup>-2</sup> at the sample position after passing through GG-420 filters. IR stimulation used an IR laser (830Δ10 nm) with a stimulation intensity of ~400 mW.cm<sup>-2</sup>. Laboratory irradiations were made using calibrated <sup>90</sup>Sr/<sup>90</sup>Y beta sources delivering about 0.10 or 0.34 Gy/s to quartz.

A heating rate of 2°C/s, unless otherwise mentioned, was used during the preheat and thermoluminescence measurements. Detection optics comprised U-340 (~99% transmission between 260 and 390 nm) filters for all quartz measurements, and a combination of BG-39 and 7-59 filters for the blue emission measurements from feldspars, both detected by an EMI 9635Q bialkali photomultiplier tube. The red emission from feldspars was measured using a combination of Comar 650IU (650±20 nm) and 650IW (650±37 nm) detection filters in front of a red sensitive GaAs photomultiplier tube (Hamamatsu R943-02) which is cooled externally by a Photocool series PMT housing (Model PC182CE).

Elemental concentrations of Uranium, Thorium and Potassium were determined using high resolution gamma spectrometry for calculation of dose rates (Murray et al., 1987).

### Results and discussion

We describe below the experiments and dosimetric results from both quartz and feldspar extracts from the studied samples. Quartz results are based on OSL and isothermal TL (ITL) measurements, while those on feldspars are based on infrared stimulated luminescence (IRSL, blue emission) and ITL (blue or red emissions) measurements.

#### *Quartz OSL and Feldspar IRSL*

The single-aliquot regenerative-dose (SAR) procedure (Murray and Wintle, 2000b) was used for quartz extracts. The signal was measured using blue light stimulation at an elevated temperature of 125°C

for 40s following a preheat of 260°C for 10s or a cutheat to 260°C. The size of the test dose was 5 Gy. OSL characteristics for sample K-IX/49 are shown in Figure 1. The OSL signal was dominated by the fast component (Figure 1a). The natural signal was in apparent charge saturation, observed to be ~150 Gy (Figure 1b). Thus the sample was beyond the OSL dating range. The growth curve was fitted using an equation of the form  $L=L_0(1-\exp-D/D_0)$  where  $L$  is the sensitivity corrected luminescence output to a given dose  $D$ , and  $L_0$  and  $D_0$  are constants. The average  $D_0$  value (this defines the curvature of the growth curve) from various aliquots of the sample was calculated to be 65 Gy suggesting that the maximum measurable dose may be about 130 Gy (at twice the  $D_0$  value, or 15% below the saturation intensity).

Although most samples were in the OSL saturation range, we also measured some younger samples on which OSL ages could be determined (Table 1). An OSL dose recovery test was carried out to confirm that a given dose on a previously unheated sample can be accurately measured in the laboratory. For sample SNG-1 the dose recovery ratio (recovered/given dose) was  $0.98\pm 0.01$  ( $n=10$ ) for a given dose of 15.6 Gy. For sample BTH-II/8 the dose recovery ratio was  $0.95\pm 0.02$  ( $n=6$ ) for a given dose of 104 Gy. These dose recovery tests suggest that there are no significant laboratory artefacts which may cause possible offsets in equivalent dose estimates. On two samples SNG-1 and BTH-II/8 the quartz ages were confirmed by AMS radiocarbon ages on carbonate shells (details in Gibling et al., 2005).

Feldspar extracts from different samples were measured using IR stimulated luminescence (in blue detection). Identical cutheat and preheat treatments, involving TL to 300°C, were carried out after various regeneration doses and a test dose of 17 Gy. Considering that the samples are old, these heat treatments were employed with an aim of sampling only the thermally stable fraction of the feldspar IRSL signal. IR stimulation was carried out at 125°C for 80s which reduced the signal to background level (Figure 1c). The natural luminescence signal was below the saturation level (average  $D_0 = 173$  Gy) in all the samples (Figure 1d).

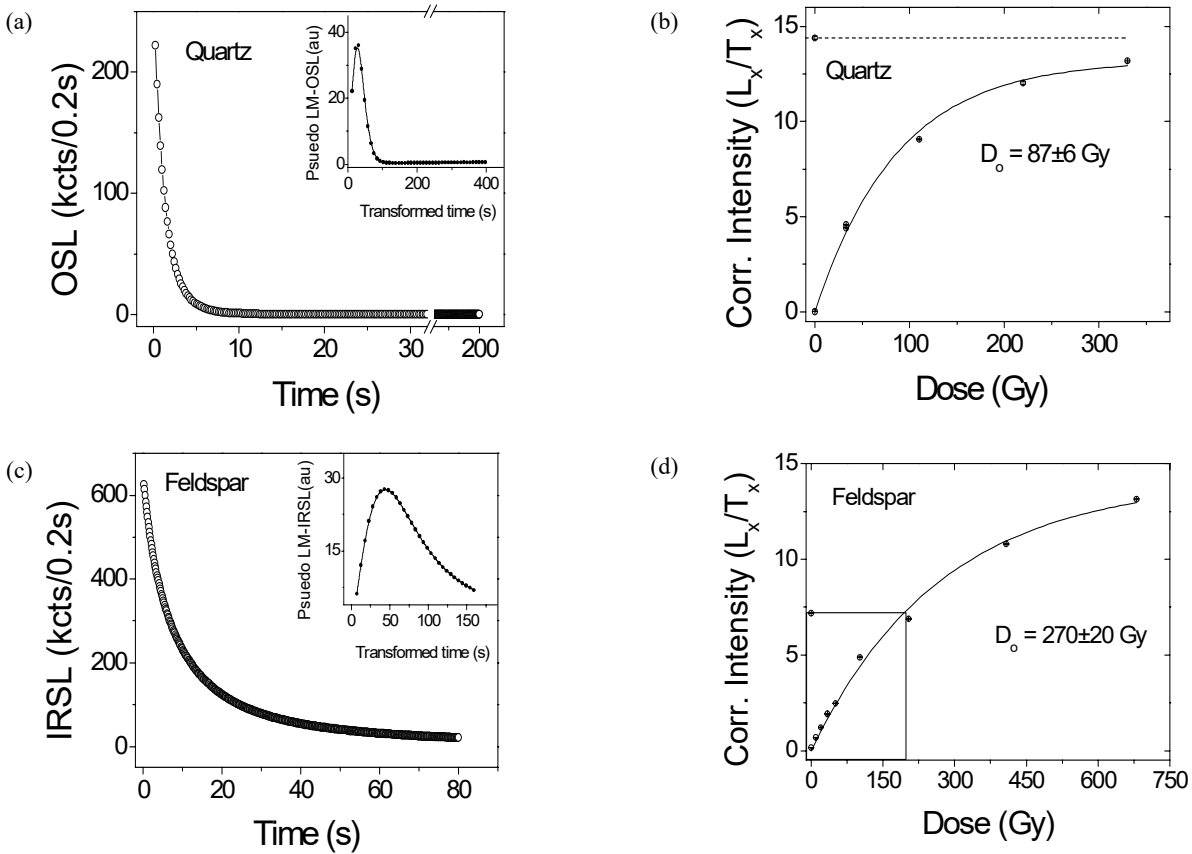


**Figure 1:** a) Natural OSL decay curve from a quartz aliquot of sample K-IX/49. The inset shows a pseudo LM-OSL curve derived from the same data. b) Dose response curve for the same aliquot of quartz. c) Natural IRSL decay curve from a feldspar aliquot of sample K-IX/49. The inset shows a pseudo LM-IRSL curve. d) Dose response curve for the same feldspar aliquot. The first 0.8s was used for signal integration in both IRSL and OSL decay curves.

A comparison of quartz OSL and feldspar IRSL ages on the five samples that were measurable by both the methods is shown in Figure 2. Feldspar doses are on average 40% lower than those from quartz; these dose differences will translate to about 50% age under-estimation when the additional internal dose rate in feldspars is taken into account (discussed

later). We attribute this under-estimation to fading, although, some differences might also occur because of errors in our dose estimation using SAR on feldspars (e.g. Wallinga et al., 2001). Since the dose underestimation is clearly systematic, it may be possible to correct for dose in older feldspar samples using a calibration based on quartz. However, in the absence of any known age older samples it is difficult to test whether such an extrapolation is meaningful or not.

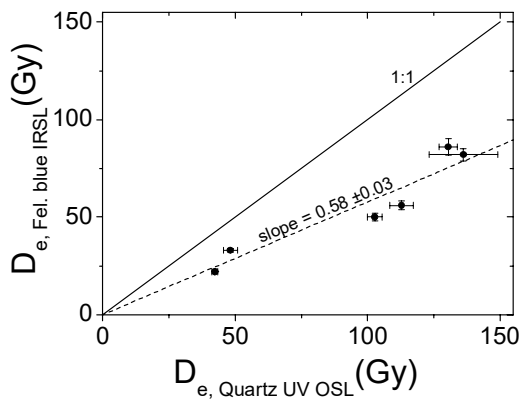


**Figure 2:** A comparison of dose estimates derived using Quartz OSL (UV emission) and Feldspar IRSL (blue emission).

**Thermoluminescence**

Results on TL investigations on quartz and feldspars are discussed below.

**Quartz: Luminescence characteristics and equivalent dose**

A TL curve obtained after a laboratory dose of 34 Gy and a preheat of 260°C for 10s is shown in Figure 3a; this curve was measured using an aliquot of the modern sample Bth (0). The curve shows a broad TL peak between 300 and 500°C. Even after heating to 500°C the composite peak is not emptied completely.

Sample	Env.	Quartz D <sub>e</sub> (Gy)		Feldspar D <sub>e</sub> (Gy)		Dose rate (Gy/ka)		Age (ka)	Quartz (ITL)	Feld (red ITL)
		OSL	ITL	Red ITL	Blue ITL	Quartz	Feldspar			
K-II/2B	F		228 ± 4	337 ± 16	273 ± 9	170 ± 7	2.9 ± 0.1		78 ± 4	101 ± 9
K-XII/4B	F		232 ± 9	373 ± 33	241 ± 9	181 ± 7	5.0 ± 0.3		47 ± 3	69 ± 8
K-XIII/4B	F	136 ± 13	138 ± 7	190 ± 18	122 ± 7	82 ± 3	3.9 ± 0.2	35 ± 4	36 ± 3	44 ± 5
K-IX/49	F		203 ± 2	404 ± 27	252 ± 4	227 ± 36	3.6 ± 0.5		57 ± 8	102 ± 17
BTh-II/8	F	113 ± 4	85 ± 2	90 ± 6	70 ± 0	56 ± 2	4.5 ± 0.3	25 ± 2	19 ± 1	18 ± 2
BTh-L1/1(3)	F	130 ± 4	133 ± 5	197 ± 15	109 ± 2	86 ± 4	4.7 ± 0.3	28 ± 2	28 ± 2	38 ± 4
BTh-II/6	F	103 ± 3	69 ± 3	83 ± 1	51 ± 2	50 ± 2	3.9 ± 0.2	26 ± 2	18 ± 1	19 ± 2
SNG-1	F	48 ± 3	59 ± 3	82 ± 3	45 ± 1	33 ± 1	3.9 ± 0.2	12 ± 1	15 ± 1	19 ± 2
DS4	A	42 ± 1	34 ± 1	33 ± 2	21 ± 1	22 ± 1	2.8 ± 0.2	15 ± 1	12 ± 1	10 ± 1
K-IX/1B	F		418 ± 35	Sat	305 ± 38	325 ± 22	3.6 ± 0.2		117 ± 11	
K-V/4	F		NM	Sat	230 ± 10	150 ± 11	3.5 ± 0.2			
K-II/4B	F		286 ± 11	336 ± 25	NM	NM	3.5 ± 0.2		82 ± 6	86 ± 9
K-II/4bU	F		216 ± 5	393 ± 15	NM	NM	3.2 ± 0.2		67 ± 4	109 ± 10
K-VII/2B	F		106 ± 9	NM	NM	NM	3.5 ± 0.2		31 ± 3	
DS-9	A	36 ± 3	31 ± 1	NM	NM	NM	3.1 ± 0.2	11 ± 1	10 ± 1	

NM – not measured

Sat. – signal in saturation

Env – Depositional environment (F – fluvial, A – Aeolian)

**Table 1:** Summary of Luminescence dating results from the samples collected from the southern Indo-Gangetic plains.

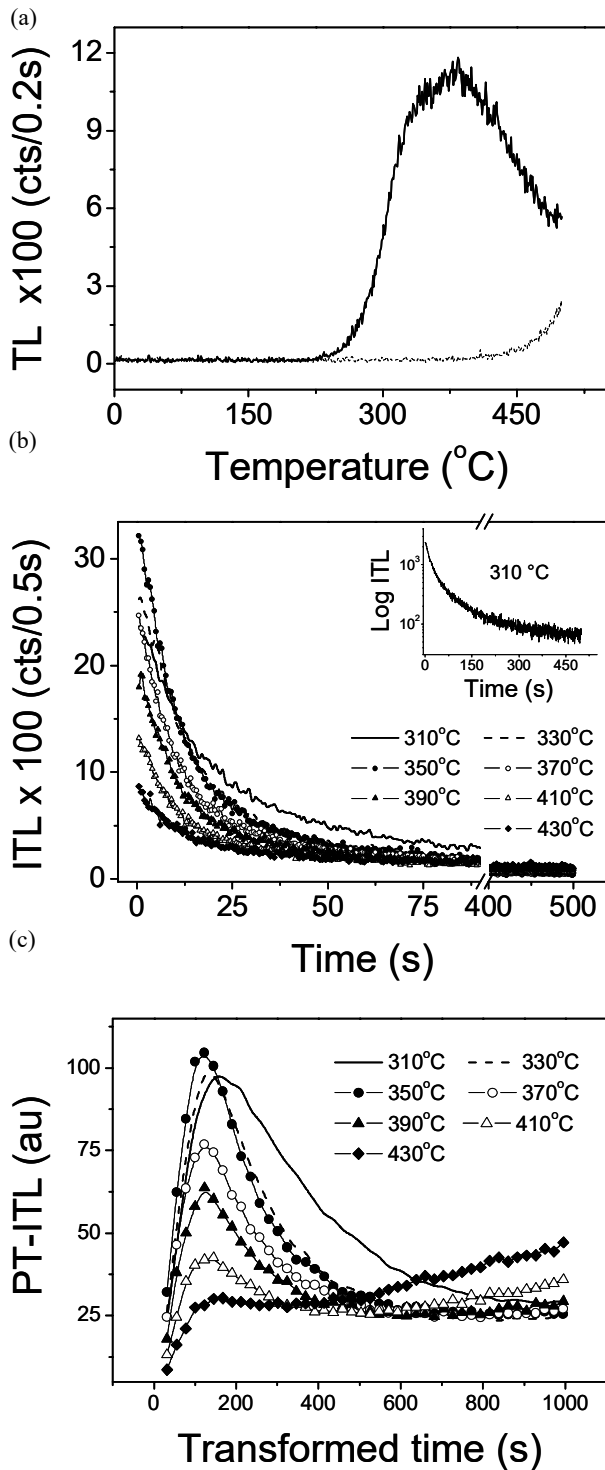


**Figure 3:** a) TL peak of an aliquot of quartz from a modern sample (BTh0) after a dose of 34 Gy and a preheat of 260°C for 10s. TL was measured at the rate of 5°C/s. The dotted curve is the repeat TL run after the TL signal had been measured. b) Natural isothermal TL decay curves measured at different temperatures c) same data plotted as peak transformed isothermal TL (PT-ITL) curves.

In a single-aliquot regenerative-dose protocol it is desirable that the signal is completely emptied after each measurement and any sensitivity change must be adequately monitored by the test dose. To satisfy the former requirement we need to heat aliquots to a high temperature in each TL based SAR cycle. For example to date using the 325°C peak one would have to heat to a high temperature such that other overlapping peaks do not contribute to the at 325°C signal during the next measurement. Such high temperature treatment may cause considerable thermally induced sensitivity changes that are not monitored accurately by the test dose. One way of keeping the heat treatment as gentle as possible is by making the measurement at a constant temperature (i.e. isothermally) just below the peak temperature of interest. This would lead to a rapid decay of the signal which would be dominated by the contribution from the TL peak just above the measurement temperature. For example, to stimulate charge from the 325°C peak it is sufficient to hold the sample at 310°C for about 90s, which reduces the signal almost to background level. A good signal separation is expected from the overlapping peaks because the measurement is made at constant temperature. In practice the heating time can be reduced even further as long as the signal is nearly emptied at the end of each cycle. Clearly this is a much less stringent heat treatment than that involved in heating the sample to beyond 500°C. In addition to good signal separation and low sensitivity changes, ITL measurement offers significant advantage in terms of thermal quenching which is constant during the measurement. Moreover, thermal quenching can be reduced by lowering the ITL temperature well below the ramped TL peak temperature, although this also reduces the rate of trap emptying.

Sample K-VII/2B was chosen for investigations of the growth behaviour of the ITL signal. The dose response at different ITL temperatures was measured using a single-aliquot regenerative-dose protocol: a) the natural signal was measured at a given temperature for 500s, b) a test dose and c) an ITL signal measurement at the same temperature as the natural signal. This cycle was then repeated for different regeneration doses. Measurement temperatures for the test dose and the regeneration doses were kept identical to make sure that the same trap has been sampled in both cases. Note that no preheating was used since by definition ITL involves heating the sample until the measurement temperature has been reached. Three aliquots were used for ITL measurement temperatures between 310 to 430°C, using 10°C increment.

Natural ITL signals from different aliquots are plotted for some representative temperatures in Figure 3b. The signals decrease as the stimulation temperature increases and all reach a background level after about 90s of stimulation. All signals show an overall non-exponential decay shape as indicated by data from ITL at 310°C on the log I scale (Figure 3b inset). It is difficult to gain insight into luminescence signal behaviour just by visual examination of a monotonously decaying signal. For a better representation, the ITL signal was converted to a peak shaped form using an arithmetic transformation suggested by Poolton et al. (2003); this transformation is based on a linear increase in the sampling time period. The peak transformed ITL (PT-ITL) signals obtained from isothermal decay curves are much more informative (Figure 3c). Some of the higher temperature PT-ITL curves show evidence for two distinct peaks, suggesting that the non-exponential nature may be caused by contribution to the signal from more than one trap. The peak time of the dominant peak decreases between 310 to 350°C (i.e. the signal decays faster), and then remains more or less constant for higher temperatures. The lack of peak shift above 350°C suggests that these curves represent data from different combinations of traps; otherwise, one would expect the peak time to decrease for higher temperature ITL stimulations.

The integrated signal over the first five seconds of the ITL decay curves was used to derive growth curves for different ITL temperatures. Growth curves were constructed by plotting the ratio between the ITL intensity of the natural or regenerated dose signal ( $L_x$ ) and the corresponding test dose signal ( $T_x$ ), as a function of the given dose. Some representative examples are shown in Figure 4a. For the 310 and 320 °C ITL signals the growth curves fit well to a single saturating exponential function with an average  $D_0$  value of 700 Gy. For measurement temperatures above 320°C, however, the  $L_x/T_x$  ratio becomes smaller at given doses > 750 Gy. Also, there is an overall drop in the  $L_x/T_x$  values for the stimulation temperatures above 370°C.

The test signal undergoes a dose dependent sensitivity increase as shown in Figure 4b where the sequence of regeneration doses is shown against the cycle number. This increase occurs above 750 Gy dose, and the maximum sensitivity change in the high temperature signal (410°C) is about ten times that in the lower temperature signal (310°C). For the intermediate temperatures it varies systematically. Whether or not this change with dose is reproducible can be tested through repeat dose points. The recycling value for the 1st and 2nd 100 Gy

regeneration doses (SAR cycles 3 and 7) is close to unity for different measurement temperatures (average =  $1.06 \pm 0.02$ ). However, the recycling value based on the 2nd and the 3rd 100 Gy dose given at the end of SAR (cycle 11) is about unity for 310 °C but then decreases systematically to about 0.4 at higher stimulation temperatures (Figure 4c) (average =  $0.63 \pm 0.05$ ). In order to check whether the poor recycling is due to changes in the  $L_x$  or in the  $T_x$  values the data are plotted in Figures 4d and 4 e for the 310 and 390°C ITL signals respectively. It can be seen that both the  $L_x$  and  $T_x$  signals show a poor recycling, however, the recycling of  $L_x$  is much poorer than that of the  $L_x/T_x$  ratio. This is perhaps because the  $T_x$  corrects for the cumulative sensitivity change prior to the  $L_x$  measurement but does not correct for those changes that occur during the measurement of the  $L_x$  signal itself. In other words, if the dose dependent sensitivity change seen in Figure 4b occurs before the regeneration ITL ( $L_x$ ) measurement then it is likely that it will be monitored by  $T_x$ . If the change, however, occurs during the  $L_x$  measurement and is dependent both on the regeneration dose and the number of repeat measurement (or SAR cycles), then poor recycling values can occur. This is perhaps an explanation for recycling data after a high dose of 750 Gy (cycles 7 and 11 in Figure 4c). A dose dependent sensitivity change occurring due to the  $L_x$  measurement implies a dip in the SAR growth curve at high doses; this is because of a large increase in the  $T_x$  values for high doses.

Another cause for the dip in the dose response curves at high temperatures may be a dose dependent shift to longer wavelengths in the emission spectra. This hypothesis, however, does not explain the poor recycling values observed in Figure 4c since the shift should be reproducible for a given dose. Therefore, based on the sensitivity change recycling data (Figures 4b and c), we consider that the dominant cause for the dip in the dose response curves may be a dose dependent sensitivity change that occurs during or towards the end of the  $L_x$  measurement at temperatures above 320°C during the ITL measurement. This causes the  $L_x/T_x$  ratio to decrease as the  $T_x$  sensitivity becomes higher than that of  $L_x$ .

Two extreme cases referring to the dose response of the 310 and 390°C ITL signals help understand this better (Figures 4d and 4e). If the test dose perfectly monitored the sensitivity of the  $L_x$  signal then the shape of the growth curve would only depend on the rate of trapped charge growth. However if the test dose is a function of the given dose and continues to increase linearly with dose, as shown in Figure 4d, then the growth curve will show a reduction in the

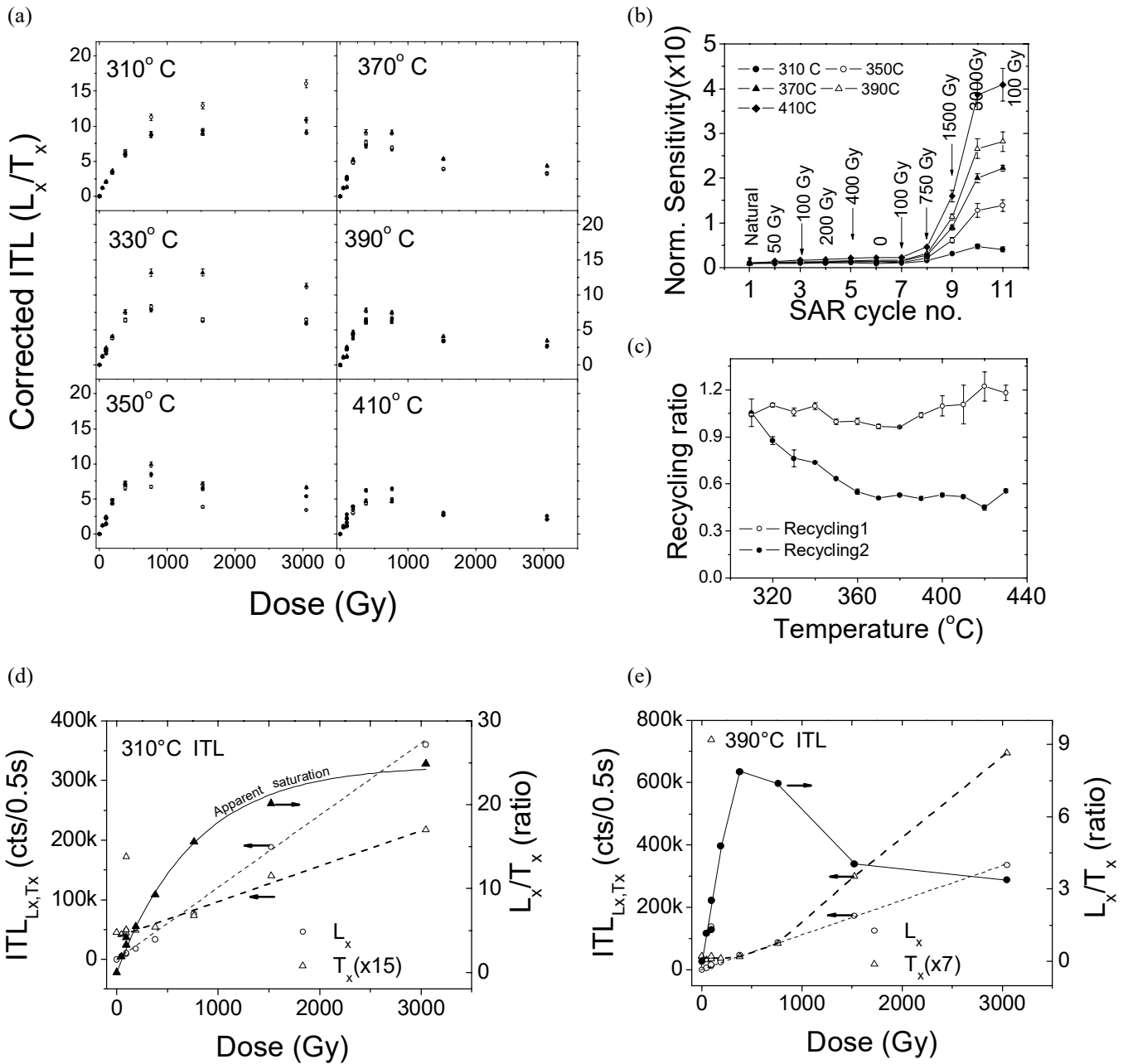


**Figure 4:** a) SAR dose–response curves for some representative ITL measurement temperatures. Three aliquots of the sample K-VII/2B were measured at each temperature. b) Normalised test dose response (with respect to the first value) as a function of SAR cycle or the corresponding regeneration dose (Gy). c) Recycling ratios calculated for the given 100 Gy regeneration doses. Recycling1 =  $ITL_{cycle\ 7}/ITL_{cycle\ 3}$  and Recycling2 =  $ITL_{cycle\ 11}/ITL_{cycle\ 7}$ . d)  $L_x$ ,  $T_x$  and  $L_x/T_x$  ratio derived from the 310°C ITL signal and plotted as a function of regeneration dose. The  $T_x$  signal has been increased by a factor of 15 so as to match the  $L_x$  signal at 750 Gy e)  $L_x$ ,  $T_x$  and  $L_x/T_x$  derived from the 390°C ITL signal and plotted as a function of regeneration dose. The  $T_x$  signal has been increased by a factor of 7 so as to match the  $L_x$  signal at 750 Gy.

$L_x/T_x$  values as the traps become saturated. In the case of the 310°C ITL signal such a charge saturation limit has not been reached within the given laboratory doses (Figure 4d). Conversely, a reduction in the  $L_x/T_x$  values will begin to occur if the test dose sensitivity rises rapidly within the given laboratory dose range. A clear example is the ITL signal at 390°C where a supralinear increase in sensitivity occurs at  $\geq 450$  Gy (Figure 4e). Such an increase causes an apparent dip in the growth curves.

These observations have an important implication for dosimetry. Since dose dependent sensitivity change also occurs at low temperature stimulations, e.g. at 310 and 320°C, although to a much lower magnitude, it is likely that the growth curves for these signals are also significantly distorted at high doses. Thus the real dose saturation level would be even higher than that indicated in the SAR growth curves (Figure 4a). A true saturation level can, however, only be observed if it is possible to measure the  $L_x$  signal without causing any sensitivity change. It is important to note that our ability to recycle an  $L_x/T_x$  ratio is good even for higher temperatures before a large dose (750 Gy) has been given (Figure 4c). The problem of growth curvature at higher temperatures, therefore, should not affect our ability to estimate  $D_e$  as long as the natural dose is below 750 Gy and the natural signal shows a similar dose dependent sensitivity change as that observed in the regeneration signals.

Equivalent doses were calculated for each stimulation temperature by interpolation of the natural to test dose ITL ratio ( $L_n/T_n$ ) on the growth curves. In most cases, the natural ratio was within the linear region of the growth curves. In Figure 5a each point represents a mean  $D_e$  value derived from three aliquots. This is plotted along with the associated standard error, and the dashed curve shows a scaled TL signal from one of the aliquots. The  $D_e$  values were about 80 - 100 Gy except for the stimulation temperatures of 350, 360 and 450°C at which they were about 150 Gy

#### Quartz: Bleaching of the ITL signal

The same aliquots described above were given a dose of 190 Gy and then bleached under the solar simulator (SOL 2) for 1 hour. After bleaching, the residual signal was treated as the natural signal and a two-cycle SAR procedure was carried out using a regenerative-dose of 190 Gy and a test dose of 37 Gy. The ITL growth curve is almost linear in this dose region (Figure 4a). For each aliquot the measurement temperature was the same as that reported in the preceding section. The residual dose for each ITL signal was calculated by interpolating the  $L_n/T_n$  ratio between the origin and the

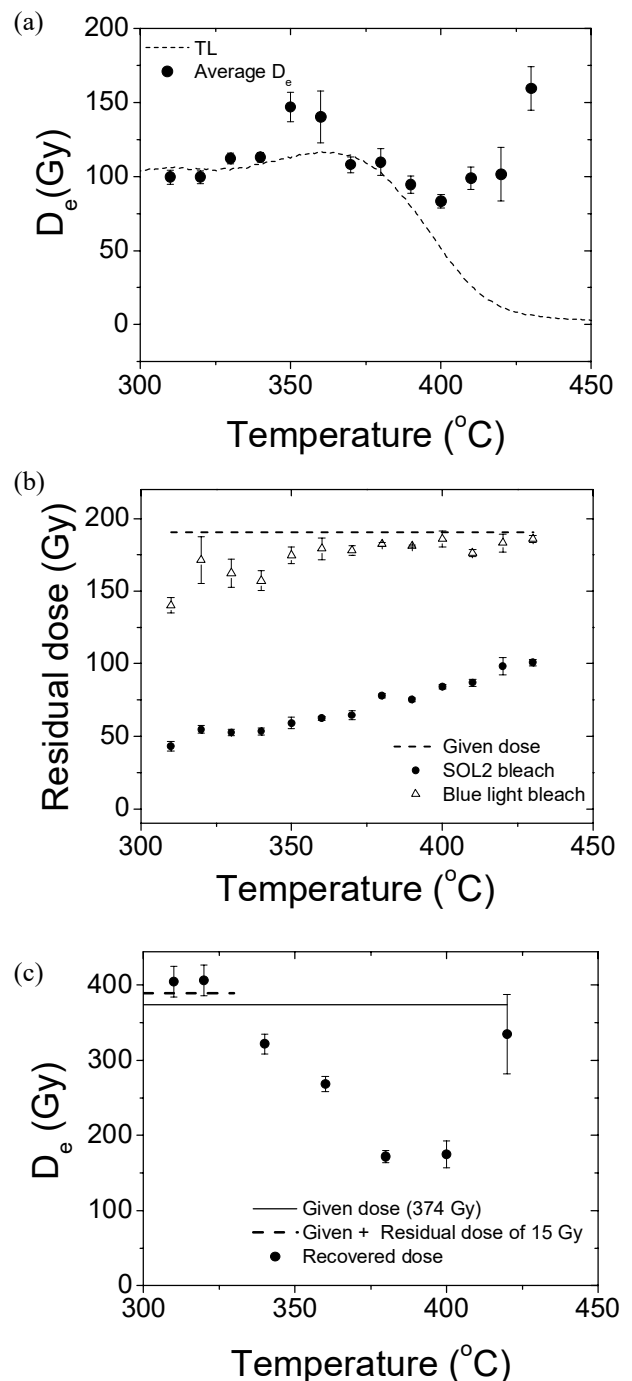


**Figure 5:** a)  $D_e$  values as a function of ITL measurement temperature for sample K-VII/2B. A scaled TL curve from the sample is also plotted to show the high temperature TL peaks. b) Residual dose after blue light or solar simulator bleaching for ITL signals measured at different temperatures. Same aliquots as those in (a) were used for the assessment of bleaching under these two light conditions. c) Dose recovery on previously unheated aliquots of the sample K-VII/2B as a function of ITL stimulation temperature.

regenerative dose point. Subsequently the same experiment was repeated except that the bleaching was carried out with blue light (470 nm) at room temperature for 1 hour. Again residual  $D_e$  values were calculated using the two-cycle SAR method as above.

The results are plotted in Figure 5b. For the ITL signal at 310°C the residual  $D_e$  after SOL2 bleaching was about 40 Gy. There was an increasing trend to about 100 Gy for higher temperature ITL signals. In the case of blue light bleaching the residual levels were much higher: ~140 Gy for the 310°C ITL signal and up to 180 Gy for higher temperatures. The amount of charge depletion was similar between 350 to 430°C.

Although the signal is measured isothermally in both the cases, the bleaching efficiency is very different for the SOL2 and blue light, especially for ITL signals between 310 and 340°C. One explanation is that the stimulation intensity under the SOL2 simulator is much higher than that under the blue light LED's, which, therefore, leads to greater depletion under the former. Alternatively, it is possible that the increased depletion is mainly due to the shorter wavelength component (< 470 nm) of the SOL2 which leads to an exponential increase in the bleaching rate (Jaek et al., 1999). We consider that the increased short wavelength component from the SOL2 is probably the main cause for increased depletion. If this interpretation is correct then it suggests that the initial ITL signals at 310 and 320°C, which are likely to be derived from the 325°C TL peak, are complex and consist of at least two traps that have similar thermal depths but markedly different optical depths. This causes the two traps to decay at a similar rate during the ITL measurement but one trap is bleachable by visible light and the other only by the short wavelength component of the SOL2 simulator. This multiple trap hypothesis is also supported by very different saturation levels of the 310°C ITL signal and the OSL signal; the latter has been shown to be related to the 325°C peak (Spooner, 1994). The complex nature of the 325°C peak has been previously suggested by Huntley et al. (1996) on the basis of depletion in the TL peak after optical exposure.

#### *Quartz: Dose recovery test*

Finally a dose recovery test was carried out on a set of fresh aliquots of sample K-VII/2B. Aliquots were bleached under the SOL2 simulator for two hours. These aliquots were then given a dose of 374 Gy. A four step SAR protocol consisting of regeneration dose, ITL measurement, test dose (50 Gy), and a further ITL measurement was carried out for some

selected temperatures. Three aliquots were used at each ITL measurement temperature. The results are plotted in Figure 5(c). The recovered dose was about 400 Gy for measurement temperatures of 310 and 320°C and then it decreased rapidly down to 175 Gy for 400°C and increased again to 334 Gy for 420°C. A ~15 Gy residual dose for the 310 and 320°C ITL signal determined on separate aliquots after two hours of SOL2 bleaching must also be taken into account. If one considers this residual dose together with the given dose (dashed line in Figure 5c) then dose estimates for the ITL temperatures of 310 and 320°C are in agreement with the known dose in the sample. For higher temperatures the dose estimates are significantly underestimated, especially if one also takes into account the higher residual levels (Figure 5b) superimposed on the given dose.

To confirm the reliability of the dose recovery for the sample under natural solar bleaching conditions, nine aliquots of sample K-VII/2B were bleached under clear daylight (in Denmark) for 1 hour. After bleaching, three aliquots were given a dose of 136 Gy and finally the dose in all nine aliquots was estimated using a four step SAR protocol using a 320°C ITL measurement temperature. The residual dose in the six bleached aliquots was estimated to be  $35.0 \pm 1.4$  Gy, which is similar to that obtained after one hour of SOL2 bleaching (Figure 5b), while that in the three dosed aliquots was  $161.7 \pm 3.4$  Gy. The recovered to given dose (including residual) ratio was calculated to be  $0.95 \pm 0.04$ .

In terms of dosimetry it appears that the 310 and 320°C ITL signals can be used for measuring the dose in quartz up to about 1400 Gy (2 times the  $D_0$  value) in our samples. For higher temperature ITL stimulations (330-350°C), there is a dose dependence in the sensitivity at high regeneration doses (>750 Gy), which causes poor recycling ratios and a dip in the dose response curves. Moreover, these higher temperature ITL signals show poorer bleaching and inaccurate dose recovery. Similar  $D_e$  values in Figure 5a for higher temperatures may perhaps be due to a combination of very poor bleaching and dose underestimation (see Figures 5b and 5c).

In the following section we test the ITL dating method on samples from the IG plains, and compare the results with quartz OSL ages, where possible.

#### *Quartz ITL at 320°C – dose measurement on natural samples*

Based on the results of our bleaching and dose recovery experiments we estimated  $D_e$  in 14 different samples using a four step SAR protocol with the ITL

signal measurement at 320°C. The results are summarized in Table 1.

Quartz OSL ages were found to be comparable with radiocarbon ages (Gibling et al., 2005). Given the good bleaching in the modern sample from the area (Jain et al., 2004) and the good dose recovery in OSL experiments, we consider that quartz OSL  $D_e$  values constitute an 'independent dose' record for assessment of the reliability of quartz ITL  $D_e$  values. A comparison of OSL and ITL  $D_e$  estimates is attempted in Figure 6. Two of the samples are aeolian (triangles), while the remaining are fluvial (circles). Most of the results fall close to a line of unit slope, even at small doses, but two fluvial samples BTH-II/6 and BTH-II/8, surprisingly, have ITL doses smaller than the OSL doses. This causes the regression line to deviate slightly from the line of unit slope (Figure 6). Since we expect that the  $D_e$  measured using ITL should be greater than or equal to that measured using OSL, the under-estimation using ITL is probably an artifact. On visual examination it was found that these two samples had a very high concentration of micas; these may give an unstable TL signal (Clark and Sanderson, 1994) and so provide one possible explanation for the age underestimation. The effect of micas on  $D_e$  estimates is however poorly understood and requires further study. Alternatively, it may be possible that the sensitivity correction of the natural signal is not working perfectly for all the samples. The recycling values show that the growth curve is very reproducible and sensitivity change is corrected for appropriately. However, if a major sensitivity change occurs during the first heating i.e. during the measurement of the natural signal then the sensitivity of the subsequent test dose ITL will be different from that of the natural ITL signal. Thus sensitivity change during the first measurement will go unmonitored and cause an offset in the  $L_n/T_n$  value. A similar

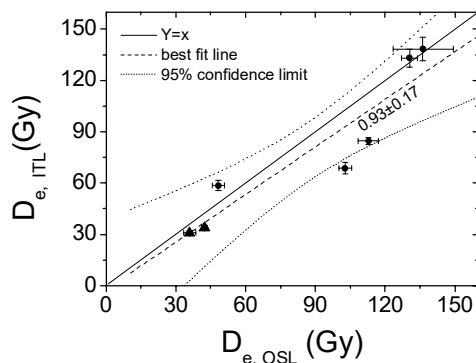


**Figure 6:** Comparison between  $D_e$  values derived using OSL and ITL signal at 320°C from quartz in some young samples.

sensitivity change during the readout of the natural OSL signal has been suggested earlier (Stokes and Singhvi, 1999; Jaiswal et al., 2004). Resolving these issues requires further investigation.

In general, the good correlation of the OSL and ITL doses, together with our previous results on dose recovery experiments, implies that the residual ITL in the natural samples, both aeolian and fluvial, were small. It is interesting to note that when close to the OSL saturation dose (~140 Gy), the spread in OSL doses is greater than that in the ITL doses (Figure 6). We consider that present results are encouraging in terms of supporting the accuracy of 320°C ITL dose estimates and their potential use in extending the age range using quartz.

For the seven samples beyond the OSL dating range, it was possible to calculate  $D_e$  values using ITL signals measured at 320°C (Table 1). This enabled us to interpret the stratigraphic evolution of one of the key areas, the Kalpi section, in the southern IG plains (Gibling et al., 2005). The maximum  $D_e$  value in our samples was 420 Gy (Table 1).

#### Feldspars

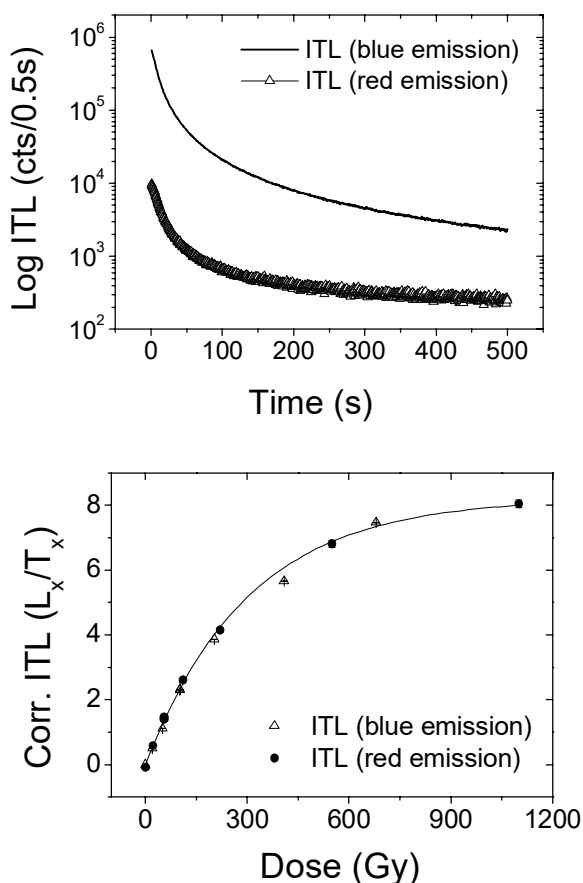
The overall level of agreement between quartz OSL and ITL doses suggests that quartz ITL (at 320°C) can be used as a dosimetric tool at higher doses. With this extension in the independent dose or age record some specific questions that can be put forward are:

- How do  $D_e$  estimates based on red and blue emission ITL from feldspars compare with those based on quartz ITL?
- How does feldspar IRSL (blue emission) compare with the blue/red emission ITL from feldspars?
- Does feldspar IRSL (blue emission) for older samples show a similar dose under-estimation as it did in the case of younger samples (Figure 2)?

These questions are addressed below.

#### Feldspar 310°C ITL (blue emission)

All feldspar ITL measurements were carried out at 310°C to make sure that a thermally stable signal was sampled. These ITL results should be directly comparable with those from IRSL obtained after preheating at 300°C. A slow non-exponential signal decay was observed and a near background level was reached in about 200s (Figure 7a). A four step SAR protocol based on an ITL measurement temperature of 310°C (for 500s) and a test dose of 34 Gy was used for dose estimation. A typical SAR growth curve obtained from these measurements is shown in



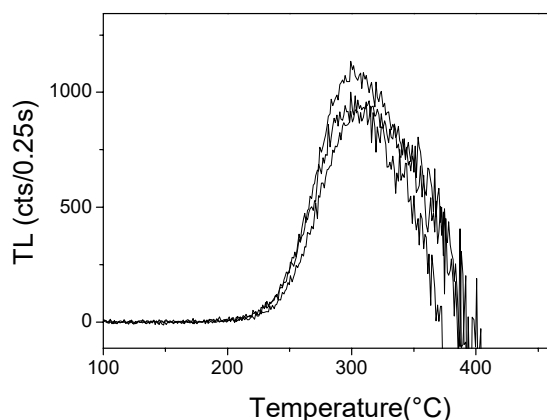
**Figure 7:** a) Blue and red emission ITL decay curves at 310°C measured from sample K-IX/49. The data is plotted on a log ITL scale. b) SAR dose response curves using blue and red ITL at 310°C.

Figure 7b fitted by a single saturating exponential growth curve. An average  $D_0$  value for different samples was 300 Gy and recycling values were within 3% of unity. The maximum  $D_e$  value was found to be 305 Gy (sample K-IX/1B), which is well below the saturation range.

#### Feldspar 310°C ITL (Red emission)

Red TL measurements from feldspars were carried out to make an assessment of fading by comparison with the previously determined  $D_e$  values using a) Quartz ITL and b) feldspar blue emission ITL. A broad peak centered at 310°C was observed (Figure 8). The isothermal TL signal at 310°C was found to be about two orders of magnitude smaller than the blue emission signal. The decay shapes, of the two signals were similar (Figure 7a).

The SAR measurement temperature was kept the same as that for the blue emission ITL, i.e. 310°C, in order to sample a geologically stable signal. Again the preheat and cutheat steps were eliminated, and the size of the test dose was 34 Gy. A typical SAR growth curve is shown in Figure 7b which is almost identical to the blue ITL growth curve in the given



**Figure 8:** Background subtracted red emission TL signal from three aliquots of the sample SNG1 containing natural dose. A heating rate of 2°C/s was used.

dose range. The average  $D_0$  value for different samples was 307 Gy. A close similarity in the dose response characteristics for identical stimulation energy (at 310°C) suggests that the blue and red ITL signals arise from the same trap. The recycling values were generally within 5% of unity suggesting a good sensitivity correction.

The maximum equivalent dose calculated using red ITL was 404 Gy for the second oldest sample K-IX/49. The Red ITL for the oldest sample K-IX/1B was in dose saturation. As seen earlier, the latter was not in dose saturation in the case of IRSL and blue ITL. We attribute this discrepancy to significantly more fading in the IRSL and blue ITL signals than in the red ITL signal, if any. Similarly sample K-V/4 was also found to be in charge saturation

#### Comparison of feldspar IRSL, blue ITL and red ITL $D_e$

On average it was observed that  $D_e$  values derived from feldspar blue ITL emission are about 18% greater than those derived using IRSL (Figure 9a). Since there appears to be a proportional relationship, except for the oldest sample K-IX/1B, a higher ITL  $D_e$  cannot be explained by poorer bleaching of the TL peak prior to deposition. If one ignores the sample, K-IX/1B which lies in the non-linear region of the growth curve, then the dose determined using IRSL is on average 34% lower than that based on blue emission ITL.

The blue ITL doses on the other hand are about 35% smaller than the red ITL  $D_e$  values (Figure 9b). As mentioned earlier, the oldest sample K-IX/1B was under charge saturation in red ITL and hence is automatically eliminated from the regression plot. These results imply that IRSL (blue emission)  $D_e$  values are on an average about 70% lower than those of the red ITL values.

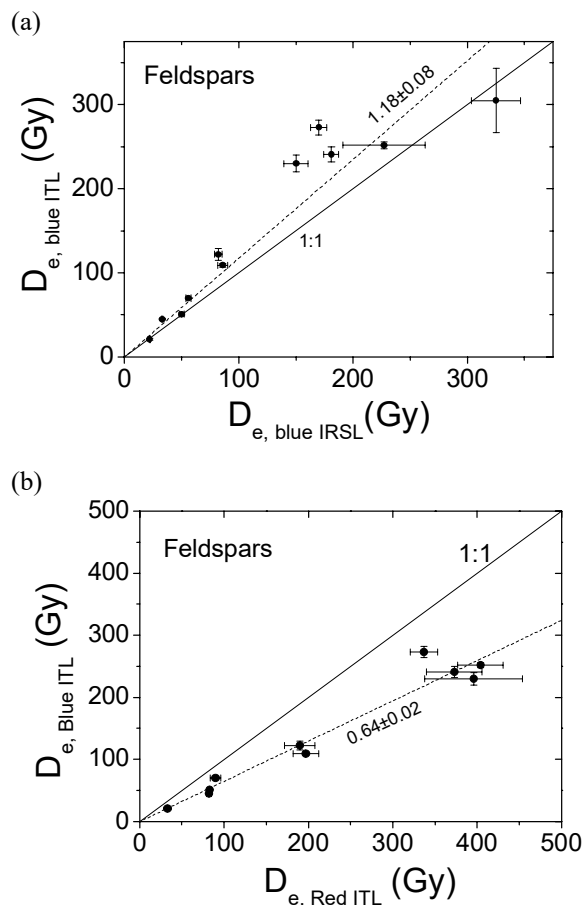


**Figure 9:** a) A comparison of  $D_e$  values derived using ITL at 310°C with those using IRSL from feldspars. Both the signals have been detected using the blue emission. b) A comparison between  $D_e$  values derived using the blue and red ITL signals measured at 310°C.

#### Comparison of $D_e$ and ages from Quartz and Feldspar

All feldspar IRSL  $D_e$  values derived previously are plotted against the corresponding quartz OSL and ITL doses in Figure 10a. The regression line indicates that feldspar  $D_e$  values are only 23% lower than those from quartz. In contrast, we had inferred that feldspar IRSL doses were about 40% lower than quartz ITL doses on the basis of  $D_e$  results from the younger samples (Figure 2). This result is contrary to our expectation since the total amount of fading should be even greater in older samples as the natural signal occurs in the more non-linear part of the growth curve. Therefore, one would expect the average dose under-estimation to increase when older samples are also considered. This dose comparison suggests that the correction factor derived from young samples cannot be simply extrapolated to the old samples.

The  $D_e$  values based on blue ITL of feldspars are similar to those from ITL of quartz except for the oldest sample K-IX/1B which forms an outlier to the general trend (Figure 10b). The datapoints generally fall on a line of slope 1. However the dose in feldspars should be higher than that in quartz because of an additional internal dose rate. The  $y=x$  trend observed here, therefore, suggests significant fading in blue emission ITL signal from feldspars.

The red ITL  $D_e$  values are on an average about 50% greater than those of quartz. However, there is a large scatter at high doses (Figure 10c). Perhaps this is because these high red ITL  $D_e$  values are well beyond the  $D_0$  value of 307 Gy. In quartz it is generally possible to measure dose accurately until about 15% of the saturation level but we are not aware of such saturation constraints on dose estimates in feldspar luminescence. If one ignores the red ITL doses above 330 Gy in the regression plot then feldspar red emission ITL doses are about 37% higher than corresponding doses in quartz.

To check if feldspar red ITL and quartz ITL ages are comparable the internal dose rate in feldspar was calculated based on  $12 \pm 0.5$  % K and  $400 \pm 100$  ppm Rb for a grain size of 100  $\mu\text{m}$  (Table 1). This contributed an additional dose rate of  $0.4 \pm 0.02$  Gy/ka to feldspars. Our calculation assumed that observed red ITL comes mainly from K-feldspars. Quartz and feldspar ages for the same samples are plotted in Figure 10d. There is a tendency for feldspar ages to be higher than quartz ages. However, except for four samples the data is consistent with a  $y=x$  relationship within  $1\sigma$  errors, and if  $2\sigma$  errors are considered then there is only one outlier to this trend. In none of the samples is a dose under-estimation in feldspars observed. If the internal feldspar dose rate is an over-estimate, then the offset between quartz and feldspar ages will be even greater than that seen in Figure 10d.

It may appear that the trend observed in Figure 10d is largely due to an absence of fading. However, a tendency to over-estimate the age using the red emission ITL from feldspars suggests that there may be an additional factor influencing the age calculation. It may be possible that there is a sensitivity change during the natural red ITL measurement which causes an increase in  $L_n/T_n$  ratio. Such a sensitivity change either does not occur in blue ITL measurements because of a different recombination centre, or the change does occur but it is not apparent due to the presence of significant fading in the blue signal. Future investigations should clarify if sensitivity change during red ITL measurements are significant or not.

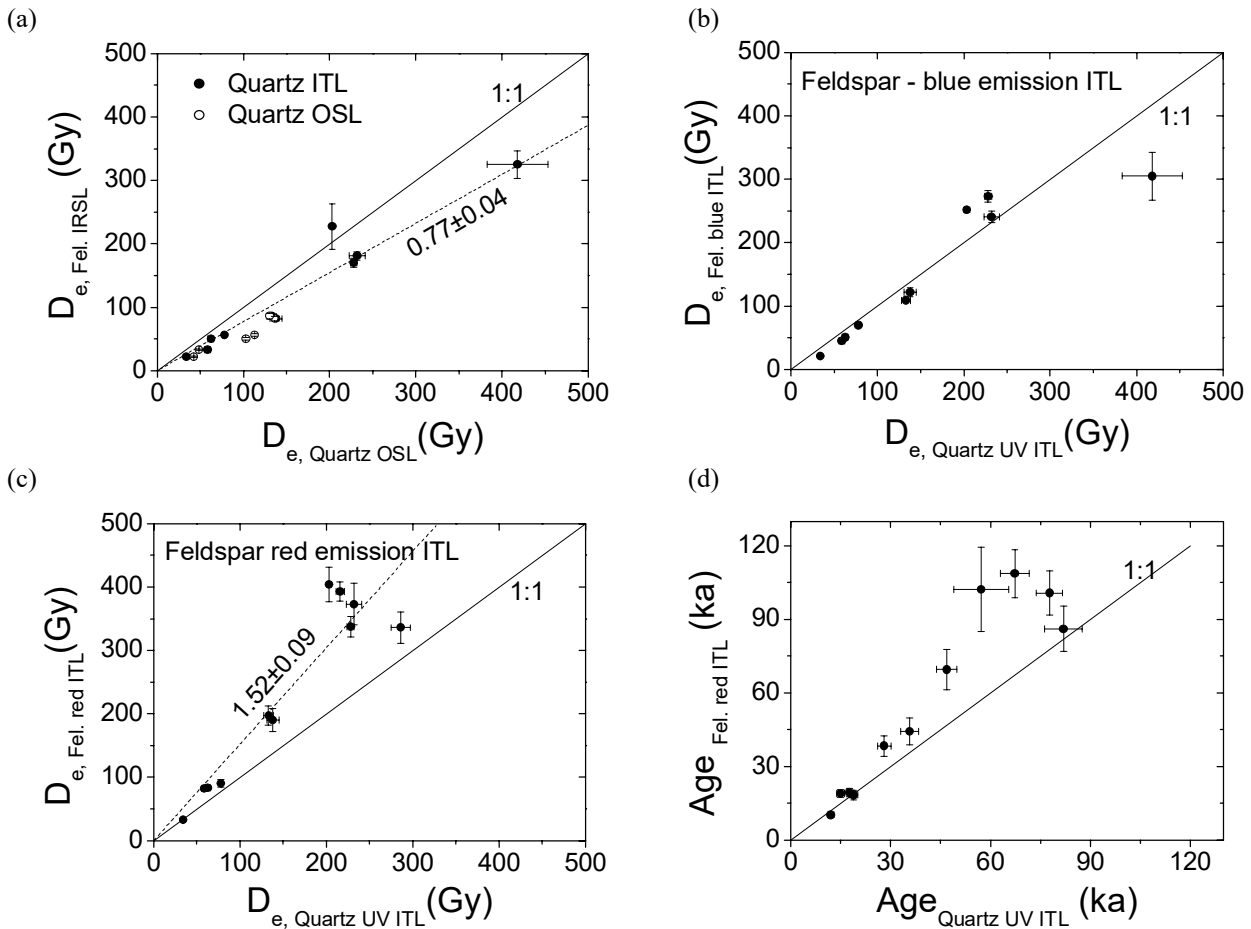


**Figure 10:** a) A comparison between  $D_e$  values derived using IRSL from feldspars, and OSL and 320°C ITL signals from quartz. b) A comparison between  $D_e$  values derived using blue emission ITL at 310°C from feldspars and UV emission ITL at 320°C from quartz. c) A comparison between  $D_e$  values derived using red emission ITL at 310°C from feldspars and UV emission ITL at 320°C from quartz. d) A comparison between feldspar red ITL and quartz ITL ages (same  $D_e$  data as (c)).

## Conclusions

The following conclusions can be made with respect to our samples from the Indo-Gangetic plains:

1. Isothermal TL signals in quartz at 310 and 320 °C offer an approach to increase the dating range. The maximum measurable  $D_e$  value using these signals is about 1.4 kGy. This is an order of magnitude increase in measurable dose as compared to quartz OSL which saturates at about 150 Gy in our samples.

2. Dose saturation levels and the bleaching data using blue or SOL2 light suggest that quartz ITL at 310 and 320°C (and therefore the 325°C TL peak) consists of traps which have similar thermal depths but significantly greater optical depths than the fast component OSL trap. Therefore there is a possibility to sample these traps using a stimulation energy

higher than that of blue light (2.6 eV) to extend the age range using an OSL method.

3. Feldspar IRSL (blue emission) may show a greater dose under-estimation than the blue emission ITL signal measured at 310°C.

4. The red emission ITL in feldspars probably suffers from sensitivity change during the measurement of the natural signal. Therefore a firm conclusion regarding fading in this signal cannot be made at present.

5. The average  $D_0$  value (saturation characteristic) calculated from SAR dose response curves on different samples is smallest for quartz OSL (~65 Gy) followed by feldspar IRSL (~173 Gy). Feldspar red and blue ITL signals at 310°C measurement temperature show similar  $D_0$  values of ~303 and

~307 Gy respectively. Quartz UV ITL shows the highest saturation level as indicated by an average  $D_0$  value of 700 Gy.

6. In feldspars the red and blue ITL signals measured at 310°C probably arise from the same trap. This is deduced from their similar dose response when measured using an identical stimulation energy (ITL at 310°C). The differences in  $D_e$  values obtained using these signals may, therefore, be caused by the fading of charge in the recombination centre and/or changes in recombination probability during the first heating for measurement of the natural signal. The latter may cause a sensitivity change that is not monitored by the natural test dose signal ( $T_n$ ).

7. Because of a lower dose rate and a higher saturation level (compared to feldspars) quartz ITL offers the best possibility to extend the luminescence dating range in samples from the southern Indo-Gangetic plains.

#### Future scope of this work

Our preliminary investigations reported here give important support for the use of TL signal in quartz to extend luminescence dating beyond the OSL range. There are several important questions raised or data unexplained which require future detailed investigations. These include:

1) What is the composition of the high temperature TL signals in quartz? Interpretation of the OSL signal as the 325°C peak appears to be a gross over simplification, although, it is not ruled out that the OSL signal may have a similar thermal depth as the 325°C peak. Our data on dose response and bleaching behaviour suggests more than one traps, in the 310-320°C ITL curves, that have different optical depths and dose saturation characteristics. A clear understanding of the kinetics of these TL signals and of thermally induced sensitivity changes during signal measurement will be important for developing widely applicable dosimetric techniques for extending the age range.

2) For widespread application of ITL SAR procedure to both quartz and feldspars, it is important to understand the nature of sensitivity change, if any, during the first measurement. This is especially important for the red TL signal from feldspars.

3) We speculate that dose dependent sensitivity change at high doses may cause an artificial curvature in the quartz ITL growth curves; this is because we expect such a sensitivity change to occur because of the  $L_x$  measurement. If this sensitivity change is associated with the recombination process

and continues to occur as a function of dose at high doses, then a dip in the growth curves is expected once the trapped charge becomes saturated after a certain dose. Thus there is a balance between trapped charge growth and recombination related sensitivity change. Although this behaviour may not have any bearing on the accuracy of dose estimates as long as natural doses are below the curve maxima (assuming that similar dose dependent sensitivity change occurs for the natural signal), or on the reproducibility of the growth curve (recycling point), it can severely limit our ability to measure high doses because of an apparent early saturation. A better understanding of dose dependent sensitivity changes and such effects requires future investigations. It is likely that such effects can also be significant in quartz OSL.

4) A better understanding of poor reproducibility in the dose response of high temperature ITL signals (>320°C) can be useful for exploiting the dosimetric potential of these signals using SAR.

5) Our preliminary data from feldspars suggests that both blue and red emission ITL signals at 310°C use the same trap. Further investigations are required to confirm this.

#### Acknowledgements

We thank Prof. A.K. Singhvi, Prof M.D. Sastry and P. Morthekai for helpful comments and a constructive review of this paper. S. Huot is thanked for calculation of internal dose rate in feldspar.

#### References

- Aitken, M. J. (1985). *Thermoluminescence Dating*. Academic Press.
- Bøtter-Jensen, L., Bulur, E., Murray, A.S. and Poolton, N.R.J. (2002). Enhancements in luminescence measurement techniques. *Radiation Protection Dosimetry* **101**, 119-124.
- Clark, R.J. and Sanderson, D.C.W. (1994). Photostimulated luminescence excitation spectroscopy of feldspars and micas. *Radiation Measurements* **23**, 641-646.
- Fattahi, M. and Stokes, S. (2000). Extending the time range of luminescence dating using red TL (RTL) from volcanic quartz. *Radiation Measurements* **32**, 479-485.
- Fattahi, M. and Stokes, S. (2003). Red luminescence from potassium feldspar for dating applications: a study of some properties relevant for dating. *Radiation Measurements* **37**, 647-660.

- Franklin, A.D. and Hornyak, W. F. (1990). Isolation of the rapidly bleaching peak in quartz TL glow curves. *Ancient TL* **8**, 29-31.
- Gibling, M.R., Tandon, S.K., Sinha, R. and Jain, M. (2005). Discontinuity-bounded alluvial sequences of the southern Gangetic plains, India: aggradation and degradation in response to monsoonal strength. *Journal Sedimentary Research* **75**, 369-385.
- Huntley, D.J. and Lamothe, M. (2001). Ubiquity of anomalous fading in K—feldspars and the measurement and correction for it in optical dating. *Canadian Journal of Earth Science* **38**, 1093–1106.
- Huntley, D.J., Short, M.A. and Dunphy, K. (1996). Deep traps in quartz and their use for optical dating. *Canadian Journal of Physics* **74**, 81-91.
- Huntley, D. J. and Prescott, J. R. (2001). Improved methodology and new thermoluminescence ages for the dune sequence in south-east South Australia. *Quaternary Science Reviews* **20**, 687-699.
- Jaek, I., Hütt, G. and Streltsov A. (1999). A study of deep traps in alkali feldspars and quartz by optically stimulated afterglow. *Radiation Protection Dosimetry* **84**, 467-470.
- Jain, M., Murray, A.S. and Bøtter-Jensen, L. (2004). Optically stimulated luminescence dating - how significant is incomplete light exposure in fluvial environments? *Quaternaire* **15**, 143-157.
- Jain, M., Tandon, S.K., Singhvi, A.K., Mishra, S. and Bhatt, S.C. (2005). Quaternary alluvial stratigraphic development in a desert setting: a case study from Luni river basin, Western India. In *Fluvial Sedimentology VII*, Eds. M. Blum and S. Marriott, Special Publication of International Association of Sedimentologists 35, 349-371.
- Jaiswal, M.K., Jain, V., Wasson, R.J., Juyal, N. and Singhvi, A.K. (2004). Luminescence characteristics of fluvial sediments from complex lithologies in Himalaya: Implications for SAR and provenance. Abstract UK luminescence and ESR meeting (September 5-8), University of St. Andrews, Scotland.
- Murray, A.S. and Olley, J.M. (2002). Precision and accuracy in the optically stimulated luminescence dating of sedimentary quartz: a status review. *Geochronometria* **21**, 1-16.
- Murray, A.S. and Wintle, A.G. (2000a). Application of the single-aliquot regenerative-dose protocol to the 375°C quartz TL signal. *Radiation Measurements* **32**, 579-583.
- Murray, A.S. and Wintle, A.G. (2000b). Luminescence dating of quartz using an improved single aliquot regenerative dose protocol. *Radiation Measurements* **32**, 57-73.
- Murray A.S., Marten, R., Johnston A. and Marten P. (1987). Analysis for naturally occurring radionuclides at environmental concentrations by gamma spectrometry, *Journal of Radioanalytical and Nuclear Chemistry* **115**, 263–288.
- Poolton, N. R. J., Bøtter-Jensen, L., Andersen, C. E., Jain, M., Murray, A.S., Malins, A.E.R. and Quinn, F.M. (2003). Measuring modulated luminescence using non-modulated stimulation: ramping the sample period. *Radiation Measurements* **37**, 639-645.
- Singarayer, J.S. and Bailey, R.M. (2003). Further investigations of the quartz optically stimulated luminescence components using linear modulation. *Radiation Measurements* **37**, 451-458.
- Spooner, N. A. (1994). On the optical dating signal from quartz. *Radiation Measurements* **23**, 593-600.
- Stokes, S. and Singhvi A.K. (1999). Personal communication.
- Wallinga, J., Murray A.S., Duller, G.A.T. and Törnqvist, T.E. (2001). Testing optically stimulated luminescence dating of sand-sized quartz and feldspar from fluvial deposits. *Earth and Planetary Science Letters* **193**, 617-630.
- Zink A.J.C. and Visocekas, R. (1997). Datability of sanidine feldspars using the near-infrared TL emission. *Radiation Measurements* **27**, 251–261.

#### Reviewer

Ashok Singhvi

#### Comments

This is an important paper with potential for older samples and should generate a lot of interest in the dating community. I also expect that the authors and others will follow up in detail as some of the observations need further probing. At present the observations intrigue me as much as they enthuse me to explore them further.

# Residual luminescence signals of recent river flood sediments: A comparison between quartz and feldspar of fine- and coarse-grain sediments

M. Fuchs, J. Straub and L. Zöller

University of Bayreuth, 95440 Bayreuth, Germany

(Received 16 March 2005; in final form 1 June 2005)

## Abstract

Sediments of the 2002 millennial flood in Saxony were investigated in respect to their residual luminescence signals. A comparison of residual palaeodoses in fine- and coarse-grain quartz and feldspar extracted from sediments was made. The fine-grain quartz was extracted by treating the sediment with  $\text{H}_2\text{SiF}_6$  that selectively dissolved fractions other than quartz. Tests using  $\text{H}_2\text{SiF}_6$  and HF for an optimum extraction of fine grain quartz were also carried out. A clear difference between quartz and feldspar based palaeodoses could be observed. Distinctly lower  $D_e$  values for quartz indicated better bleaching. Residual  $D_e$  values ranged from 0.5 Gy to 16 Gy for fine-grain quartz and coarse-grain K-feldspars, respectively.

**Keywords:** residual doses, bleaching, fluvial deposits

## Introduction

One of the problems in optical dating of fluvial sediments is the confirmation of the extant of optical resetting of the geological luminescence signal at the time of deposition and burial (e.g. Fuchs and Lang, 2001; Olley et al., 1998; Stokes et al., 2001). The process of resetting strongly depends on the mineral type, the spectral quality and fluence of daylight. For a given spectrum, the quartz luminescence bleaches faster than that of feldspars (Godfrey-Smith et al., 1988). The daylight spectrum depends on the filtering and attenuation of the solar spectrum in water i.e. the depth and sediment load of the river (Berger, 1990; Ditlefsen, 1992). The foregoing implies that the bleaching characteristics of the grains should be dependent on the grain size since different grain sizes are transported differently. Typically the finer silt size fraction is more likely to be transported in suspension (i.e. closer to the water air- interface). In contrast, the sand and coarse silt fraction settle more quickly within the water column and are transported mostly as bed loads. Thus, there should be a higher

probability of a better daylight-bleaching of the fine silt fraction. A complicating factor is that grains of the fine silt fraction tend to coagulate to form larger aggregates (Kadereit, 2000; Lang 1996), behaving like sand sized grains during their fluvial transportation and sedimentation. The grains within these aggregates are shielded from daylight by the outer grains and therefore tend to be insufficiently bleached.

Based on these considerations, sediments from the millennial flood in August 2002 in Saxony, Germany, were investigated in respect of their residual luminescence signals (Straub, 2004). Ideally, for these sediments equivalent doses should be close to zero, if sufficient bleaching of the sediments during their last reworking occurred. The extent of bleaching of different mineral types (quartz and feldspar) and different grain sizes (coarse- and fine-grain) were investigated.

## Materials and methods

Fluvial sediments from the catastrophic 2002 flooding event at the rivers Elbe and Rote Weißeritz in Saxony, Germany, were investigated. Four fine-grained backswamp sediments from the river Elbe were taken north of Dresden (EL2: N51°03'53.88'', E13°43'53.55'', 110 m a.s.l.; EL5,6,7: N51°05'50.32'', E13°39'01.23'', 110 m a.s.l.), where the upstream catchment area is ca. 53,000 km<sup>2</sup>. Sediments consisting almost entirely of sand-sized material from the river Rote Weißeritz, a tributary to the river Elbe, were sampled from a fresh point-bar (N50°57'3.76'', E13°38'3.76'', 300 m a.s.l.) in the V-shaped valley near Seifersdorf (Ore Mountains) at the upper part of the catchment, 1.5 km downstream of a dam. From this site, three samples (RW3, RW4, RW5) were taken (Figure 1). Sediments from both sites were sampled a few weeks after the flooding event.

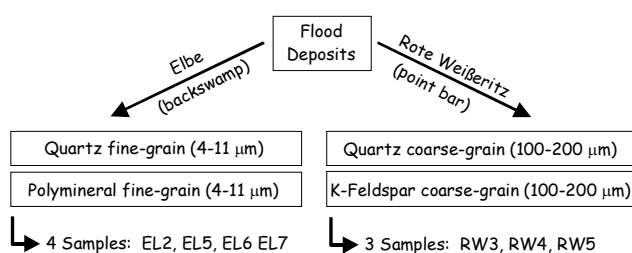


**Figure 1:** Sediment samples from the river Elbe and Rote Weißeritz. From the river Elbe four fine-grain samples were investigated, from the river Rote Weißeritz three coarse-grain samples. From both rivers quartz and feldspars were used for  $D_e$  determination.

For luminescence measurements, quartz and K-feldspar minerals of the coarse-grain fraction (100-200 µm) from the river Rote Weißeritz were extracted, using standard techniques. The polymineral and quartz fine-grain fractions (4-11 µm) were extracted from the deposits of the river Elbe (Figure 1). To separate the fine-grain quartz fraction, the techniques suggested by Prasad (2000) using hydrofluoric acid (HF), by Jackson et al. (1976) and by Berger et al. (1980) using fluorosilicic acid ( $H_2SiF_6$ ) were tested. The procedure suggested by Prasad (2000) was found to be insufficient as after etching in 5 % and 10 % HF for 80 minutes and 120 minutes significant feldspar could still be detected by IRSL and X-ray diffraction. Etching with pre-treated 34 %  $H_2SiF_6$  was carried out after Berger et al. (1980), varying the pre-treatment time, the etching time with its stirring frequency and the acid / sample ratio (Table 1). The pre-treatment of  $H_2SiF_6$  was carried out by adding commercial quartz (100-500 µm) to the acid at a ratio of 1:10 and occasionally stirring the mixture. After pre-treatment for 3 or 7 days, the commercial quartz was filtered out and the acid was then used for etching the sediment samples. Optimum results in the extraction of fine-grain quartz were obtained by using  $H_2SiF_6$  pre-treated for 3 days, etching each sample twice for 3 days (with a washing step in between), and stirring the samples twice per day. The loss in the weight of the sediment after this procedure was circa 74 % - 79 % (Table 1). The purity of the quartz fine-grain extracts was tested by IRSL and X-ray diffraction (Mauz and Lang 2004). Absence of any IRSL signal indicated the high purity of the fine-grain quartz extracts.

To determine the equivalent doses ( $D_e$ ) a single aliquot regeneration (SAR) protocol (Murray and Wintle 2000) was used for the quartz fraction. A single aliquot regeneration protocol was used for the K-feldspar and polymineral fraction (Kadereit 2000).

Typically up to 15 aliquots per sample were measured for  $D_e$  determination. Although 15 aliquots is too low a number for reliable estimation of  $D_e$  in dating applications, we feel that it is sufficient to get an order of magnitude estimate of the equivalent dose from such poorly bleached flood sediments.

Pre-treatment <sup>1</sup>	Stirring-time <sup>2</sup>	Ratio <sup>3</sup> Sediment / $H_2SiF_6$	Loss <sup>4</sup> [%]
3 days	continuous	1:40	No yield
7 days	continuous	1:40	No yield
3 days	continuous	1:40	98
7 days	continuous	1:40	98
0 days	2 times / day	1:20	No yield
3 days	2 times / day	1:40	84
7 days	2 times / day	1:40	89
3 days	2 times / day	1:20	72
3 days	2 times / day	1:20	79
3 days	2 times / day	1:20	76
3 days	2 times / day	1:20	74
3 days	2 times / day	1:20	75

**Table 1:**  $H_2SiF_6$  etch procedures to extract fine-grain quartz from fluvial sediments.

<sup>1</sup>  $H_2SiF_6$  pre-treatment with commercial quartz (100-500 µm) with a quartz:acid ratio of 1:10

<sup>2</sup> during sample etching with pre-treated  $H_2SiF_6$

<sup>3</sup> ratio between sediment extract and  $H_2SiF_6$  while etching

<sup>4</sup> Sediment loss after etching

Optically stimulated luminescence from the quartz samples was measured for 20 s, using the first 0.4 s of the measurement for  $D_e$  determination, and subtracting a background signal from 16-20 s. For the polymineral and feldspar samples luminescence was measured for 240 s, using the first 100 s for  $D_e$  determination, and subtracting a background signal from 200-240 s. Typical quartz (OSL) and polymineral (IRSL) decay curves of the fine-grain fraction (EL5) are shown in Figure 2.

Luminescence measurements were carried out on a Risø Reader TL-DA-15. Quartz extracts were stimulated at 125°C with blue light (470 Δ 20 nm; ca. 36 mW/cm<sup>2</sup>) and detected in the 290-370 nm (Hoya U340) wavelength band. The K-feldspar and polymineral extracts were stimulated at room temperature with infrared (875 Δ 80 nm; ca. 67 mW/cm<sup>2</sup>) and detected in the 390-450 nm (Schott BG39, 2 x BG3, GG400) wavelength band, as recommended by Krbetschek et al. (1996).

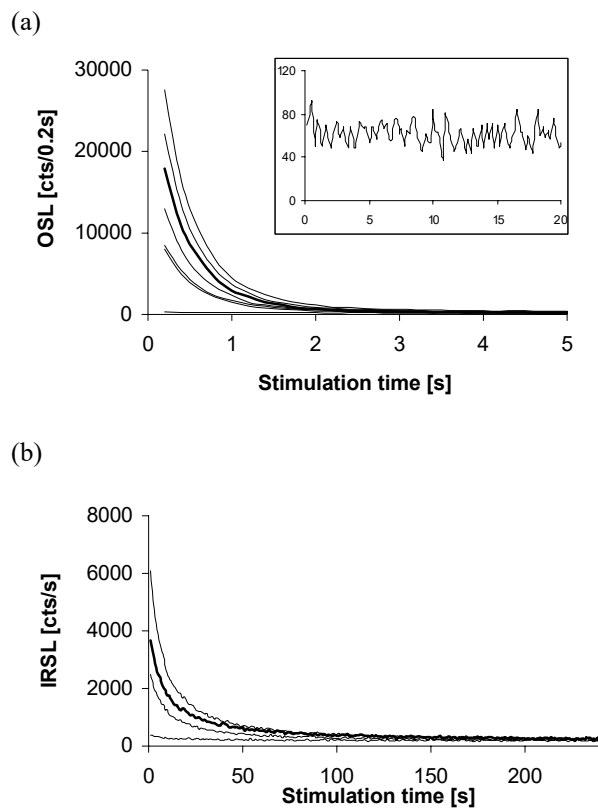


**Figure 2:** OSL and IRSL decay curves for sample EL5 (figure a: quartz fine grains; figure b: polymineral fine grains). The graphs show the decay curves of the natural signal (bold line) and the regenerated signals. Inset of figure a: IRSL stimulated signal of the quartz fine grain fraction. The sample shows no IRSL signal, thus no feldspar contamination (for axis labels see large figure).

### Results and discussion

In Table 2 results of the equivalent dose determination ( $D_e$ ) along with their standard deviation are given for the samples from the rivers Elbe (fine-grain) and Rote Weißeritz (coarse-grain). All samples show a  $D_e > 0$ , regardless of the grain size or mineral fraction used for  $D_e$  determination.

The expected zero value for recently deposited sediments was not found. An indication of insufficient bleaching is also given by the high scatter of  $D_e$  values for the coarse-grain samples, expressed as the standard deviation. This is due to the number of grains per measured aliquot (ca. 500), which consist of heterogeneously bleached grains. The measured fine-grain aliquots do not show this high scatter, because of the much larger number of grains per aliquot (ca. 14,000) that averages out the heterogeneity (Fuchs and Wagner, 2003). Examples of dose distributions for coarse- and fine-grain quartz samples are given in Figure 3.

Sample	Mineral	$D_e$ [Gy]	SD [Gy]	SD [%]
<i>Fine-Grain (Elbe)</i>				
EL2	Quartz	0.50	0.07	14
EL5	Quartz	0.75	0.06	8
EL6	Quartz	1.57	0.17	11
EL7	Quartz	1.32	0.11	8
EL2	Polyminerals	5.81	0.45	8
EL5	Polyminerals	4.49	0.28	6
EL6	Polyminerals	16.03	0.60	4
EL7	Polyminerals	10.19	0.65	6
<i>Coarse-Grain (Rote Weißeritz)</i>				
RW3	Quartz	2.32	1.43	62
RW4	Quartz	1.00	0.27	27
RW5	Quartz	1.67	0.49	29
RW3	Feldspar	7.41	8.75	118
RW4	Feldspar	7.72	6.64	86
RW5	Feldspar	16.35	17.90	109

**Table 2:** Mean equivalent doses ( $D_e$ ) of recent river flood sediments from the river Elbe and Rote Weißeritz for the minerals quartz and feldspar.  $D_e$  values are given with their standard deviation (SD).

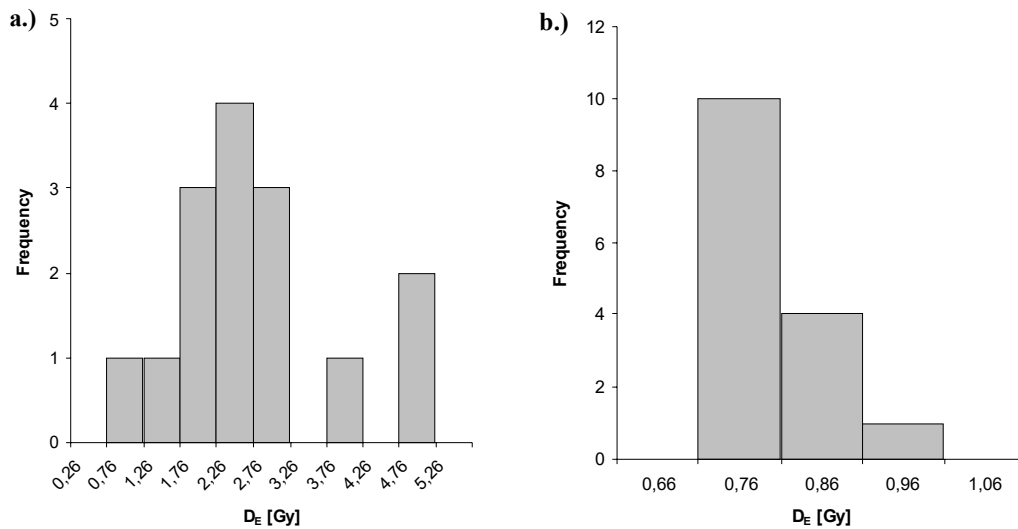


**Figure 3:** Examples of typical dose distributions from coarse- (RW3, figure a) and fine-grain (EL5, figure b) quartz samples. Due to the small number of grains on the coarse grain aliquots (ca. 500) the distribution is much broader than that of the fine grain aliquots which have ca. 14,000 grains per aliquot.

Even though none of the samples show a zero  $D_e$ , there are differences in the degree of luminescence signal resetting between the quartz and feldspar fraction of the fine- and coarse-grain extracts. Based on the values given in table 2,  $D_e$  values of feldspar and quartz are compared in Figure 4. Both, the fine- and coarse-grain quartz fractions are better bleached than the corresponding feldspar fractions. In the case of coarse grains, quartz shows a 3-10 times lower  $D_e$  than feldspar. For fine grains the differences in  $D_e$  values are even larger and quartz is showing an 8-12 times lower  $D_e$  than feldspar of the polymineral fraction. These large differences are higher than the difference due to the internal  $\beta$  dose rate of coarse K-feldspar grains ( $\sim 0.5$  Gy/a) or a lower  $a$ -value for fine quartz grains (typically ca. 0.03 rather than ca. 0.08 for feldspars), respectively. As residual  $D_e$  values rather than apparent ages were the purpose of this study, dose-rate measurements were not carried out from the samples. Assuming effective dose-rates of ca. 4 mGy/a for feldspar fine grains, ca. 3.5 mGy/a for quartz fine grains and for K-feldspar coarse grains and ca. 2.8 mGy/a for quartz coarse grains the following values would result as “residual” ages:

- Elbe-samples quartz fine grains:  
0.14 to 0.45 ka
- Elbe-samples feldspar fine grains:  
1.12 to 4.0 ka
- Rote-Weißeritz-samples quartz coarse grains:  
0.36 to 0.83 ka
- Rote Weißeritz-samples K-feldspar coarse grains:  
2.12 to 4.67 ka

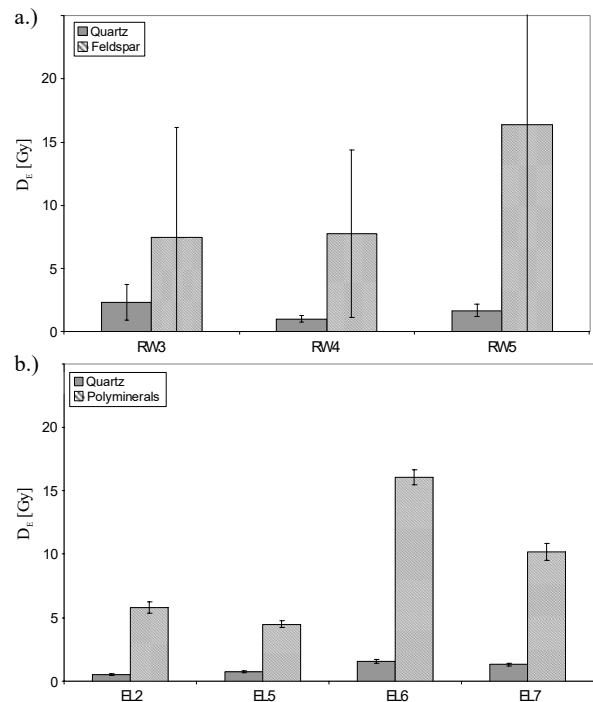


**Figure 4:** Comparison of residual equivalent doses between quartz and feldspar ( $D_e$ ) from recent river flood sediments from (a) Rote Weißeritz and (b) the river Elbe.  $D_e$  error bars are quoted at the  $1\sigma$  level.

We emphasize, however, that these values can only be taken as approximate first order estimates of apparent ages and indicate the amount of zero error in dating older samples of similar depositional history.

A comparison of different grain sizes for the same mineral is difficult, because there was not sufficient fine- and coarse-grain material available from the same samples. However, comparing quartz and feldspar of the fine- and coarse-grain fractions, there seems to be a trend towards lower  $D_e$  values for the fine-grains (Table 1, Figure 3). This could also be explained by extended transportation and thus better bleaching of the fine-grain sediment from the river Elbe in comparison to the coarse-grains from the river Rote Weißeritz. In the case of the Elbe site, the distance between the upper drainage system and the sample locality is some orders of magnitude larger than that of the Rote Weißeritz site (cf. Stokes et al., 2001).

### Conclusion

Fine-grain (4-11  $\mu\text{m}$ ) quartz could be successfully extracted from the Elbe sediments by etching the polymineral fine-grain fraction with  $\text{H}_2\text{SiF}_6$ . Etching with HF as suggested by Prasad (2000) was not successful. Regardless of the minerals or grain sizes used for  $D_e$  evaluation, no zero  $D_e$  values could be obtained for recently deposited sediments. This is explained by insufficient bleaching of the sediments. Quartz showed considerably lower  $D_e$  values than feldspar, and could be used for optical dating of such sediments from catastrophic floods. Typical 'zero error' on age is estimated so as to provide an estimate of the amount of uncertainty associated with older sediment of similar depositional history. The present study suggests that the 'zero-error' in dating such catastrophic flood events in the region will be in the order of 0.1 to 1 ka for quartz and 1 to 5 ka for feldspars, respectively.

### Acknowledgements

We would like to thank Prof. A.K. Singhvi for discussion and helpful comments.

### References

- Berger, G.W., Mulhern P.J. and Huntley, D.J. (1980). Isolation of silt-sized quartz from sediments. *Ancient TL* **11**, 8-9.
- Berger, G.W. (1990). Effectiveness of natural zeroing of the thermoluminescence in sediments. *Journal of Geophysical Research* **95**, 12375-12397.
- Ditlefsen, C. (1992). Bleaching of K-feldspars in turbid water suspensions: A comparison of photo- and thermoluminescence signals. *Quaternary Science Reviews* **11**, 33-38.
- Fuchs, M. and Lang, A. (2001). OSL dating of coarse-grain fluvial quartz using single-aliquot protocols on sediments from NE Peloponnese, Greece. *Quaternary Science Reviews* **20**, 783-787.
- Fuchs, M. and Wagner, G.A. (2003). Recognition of insufficient bleaching by small aliquots of quartz for reconstructing soil erosion in Greece. *Quaternary Science Reviews* **22**, 1161-1167.
- Godfrey-Smith D.I., Huntley, D.J. and Chen, W.-H. (1988). Optical dating studies of quartz and feldspar sediment extracts. *Quaternary Science Reviews* **7**, 373-380.
- Jackson, M.L., Sayin, M. and Clayton, R.N. (1976). Hexafluorosilicic acid reagent modification for quartz isolation. *Soil. Sci. Am. J.* **40**, 958-960.
- Kadereit, A. (2000). *IR-OSL-datierte Kolluvien als Archive zur Rekonstruktion anthropogen bedingter Landschaftsveränderungen*. Ibidem-Verlag, Stuttgart.
- Krbetschek, M.R., Rieser, U. and Stolz, W. (1996). Optical dating: Some luminescence properties of natural feldspars. *Radiation Protection Dosimetry* **66**, 407-412.
- Lang, A. (1996). *Die Infrarot-Stimulierte Lumineszenz als Datierungsmethode für holozäne Lössderivate*. PhD thesis, University of Heidelberg, 137pp.
- Mauz, B. and Lang, A. (2004). Removal of the feldspar-derived luminescence component from polymineral fine silt samples for optical dating applications: evaluation of chemical treatment protocols and quality control procedures. *Ancient TL* **22**, 1-8.
- Murray, A.S. and Wintle, A.G. (2000). Luminescence dating of quartz using an improved single-aliquot regenerative-dose protocol. *Radiation Measurements* **32**, 57-73.
- Olley, J., Caitcheon, G. and Murray, A.S. (1998). The distribution of apparent dose as determined by optically stimulated luminescence in small aliquots of fluvial quartz: Implications for dating young sediments. *Quaternary Geochronology* **17**, 1033-1040.

- Prasad, S. (2000). HF treatment for the isolation of fine grain quartz for luminescence dating. *Ancient TL* **18**, 15-17.
- Stokes, S., Bray, H.E. and Blum, M.D. (2001). Optical resetting in large drainage basins: tests of zeroing assumptions using single-aliquot procedures. *Quaternary Science Reviews* **20**, 879-885.
- Straub, J. (2004). *Studien zur Datierung von Hochflutsedimenten mittels Optisch-Stimulierter Lumineszenz am Beispiel von Ablagerungen der Flutkatastrophe in Sachsen 2002*. Unp. Dipl. Thesis. University of Bayreuth, Germany.

**Reviewer**

Ashok Singhvi

**Comments**

This study provides useful new data that will be of potential use in future studies on fluvial systems in the region.

## Thesis Abstract

---

**Author:** George James Susino  
**Thesis Title:** Analysis of lithic artefact microdebitage for chronological determination of archaeological sites  
**Grade:** PhD  
**Date:** October 2004  
**Supervisors:** Richard G. Roberts, Lesley Head and Deirdre Dragovich  
**Address:** University of Wollongong, GeoQuEST Research Centre, School of Earth and Environmental Sciences, Australia

This study explores the use of several different techniques to isolate and determine the age of lithic microdebitage in relation to archaeological deposits and associated sediments. Quartz microdebitage was identified on the basis of surface features and roundness index by applying scanning electron microscopy (SEM) and optical stereomicroscopy to archaeologically relevant sediments. Characteristics of the quartz microdebitage were compared with quartz grains from the same sedimentary layer. The observation of diagnostic features on quartz grains made it possible to discriminate between microdebitage and sedimentary background.

This investigation has established that microdebitage particles under 500  $\mu\text{m}$  diameter are not easily resolved under optical stereomicroscopy, requiring the aid of SEM to discern between microdebitage and sedimentary quartz. It was also ascertained that no adverse effects on the optically stimulated luminescence (OSL) signal are measurable after exposure to SEM, provided that the electron beam is kept at, or under, 10 keV.

Sedimentary material previously excavated from the Jinnium rockshelter (Northern Territory) and Mushroom Rock West (Queensland) was used to determine the age of quartz microdebitage from the archaeological layers by applying the OSL dating technique. The microdebitage OSL signal behaves similarly to that of sedimentary quartz grains, and is subject to the same problems. The OSL single-aliquot regenerative-dose protocol (SAR) was successfully applied to the age determination of microdebitage. The modifications used for the dose

rate (due to particle size and shape) and for the calibration of the beta source (due to particle size) did not produce any inconsistencies or anomalous results. In the investigation of two archaeologically relevant sediment layers from the Jinnium rockshelter deposit, the minimum OSL age at 68 cm depth for the microdebitage was estimated as  $4100 \pm 900$  years ( $12,600 \pm 4000$  years using the central age model estimate, with 73% over-dispersion on the palaeodose), and, for the sedimentary material, a central age model of  $5300 \pm 800$  years (with a minimum age model estimate of  $1900 \pm 400$  years, and, 78% over-dispersion). At 115 cm in the deposit, the OSL central age model estimate for the microdebitage is  $10,200 \pm 1100$  years, with a minimum age model of  $4500 \pm 600$  years (and an over-dispersion of 56%). In the case study of Mushroom Rock West rockshelter, the OSL central age model estimate for microdebitage at 268 cm depth into the archaeological deposit is  $21,200 \pm 3100$  years (with a minimum age model estimate of  $10,500 \pm 5200$  years, and 60% over-dispersion), compared to a central age model estimate for the sedimentary quartz grains of  $31,500 \pm 3100$  years (with a minimum age model estimate of  $11,100 \pm 1500$  years, and 67% over-dispersion). For the archaeological layer situated at 441 cm depth, the microdebitage yielded an OSL age of  $27,400 \pm 2200$  years. This sample of microdebitage produced the lowest over-dispersion (0.1%) on the palaeodose of any of the samples analysed, lending confidence to the accuracy of the palaeodose determination. The sedimentary quartz from the same sample produced an OSL minimum age model estimate of  $33,500 \pm 5600$  years (and a central age model estimate of  $46,900 \pm 3400$  years). Relationships between microdebitage and sediment OSL ages are discussed.

Direct OSL dating of the unheated quartz derived from the manufacture of lithic tools now provides an alternative to the reliance on sedimentary quartz as the primary source information regarding the age of archaeological deposits. This knowledge may be applied also to archaeological sediments previously excavated, for identifying episodes of lithic manufacture in temporal relation to other evidence of cultural activity. The ages of the two archaeological sites analysed differ widely, and this difference was also represented in the ages obtained from the microdebitage. None of the OSL age determinations of microdebitage was found to be unrealistically outside the boundaries of pre-existing age control.

This is one indication of the validity of the novel experimental approach applied.

Copies of the thesis are held at: University of Wollongong Library; School of Earth and Environmental Sciences (University of Wollongong); and in digital format through the Australian Digital Theses Program (<http://adt.caul.edu.au/>). The thesis is also available from the author in pdf format upon request (E-mail: [george@rockart.wits.ac.za](mailto:george@rockart.wits.ac.za)).

## Bibliography

### Compiled by Ann Wintle

---

#### From 1st January 2005 to 30th June 2005

- Adrielssohn, L., and Alexanderson, H. (2005). Interactions between the Greenland Ice Sheet and the Liverpool Land coastal ice cap during the last two glaciation cycles. *Journal of Quaternary Science* **20**, 269-283.
- Alexandrescu, E., Balescu, S., and Tuffreau, A. (2004). New chronological, technological and typological data on the Early Upper Palaeolithic of the Romanian Danube Plain: the Giurgiu-Malu Rosu site (in French). *Anthropologie* **108**, 407-423.
- Argilyan, E. P., Forman, S. L., Johnston, J. W., and Wilcox, D. A. (2005). Optically stimulated luminescence dating of Late Holocene raised strandplain sequences adjacent to Lakes Michigan and Superior, upper peninsula, Michigan, USA. *Quaternary Research* **63**, 122-135.
- Bailey, R. M., Armitage, S. J., and Stokes, S. (2005). An investigation of pulsed-irradiation regeneration of quartz OSL and its implications for the precision and accuracy of optical dating (Paper II). *Radiation Measurements* **39**, 347-359.
- Blair, M. W., Yukihiro, E. G., and McKeever, S. W. S. (2005). Experiences with single-aliquot OSL procedures using coarse-grain feldspars. *Radiation Measurements* **39**, 361-374.
- Bokhorst, M. P., Duller, G. A. T., and Van Mourik, J. M. (2005). Optical dating of a Fimic Anthrosol in the southern Netherlands. *Journal of Archaeological Science* **32**, 547-533.
- Bristow, C. S., Lancaster, N., and Duller, G. A. T. (2005). Combining ground penetrating radar surveys and optical dating to determine dune migration in Namibia. *Journal of the Geological Society, London* **162**, 315-321.
- Cannas, M., Agnello, S., Gelardi, F. M., Boscaino, R., Trukhin, A. N., Liblik, P., Luschik, C., Kink, M. F., Maksimov, Y., and Kink, R. A. (2004). Luminescence of gamma-radiation-induced defects in alpha-quartz. *Journal of Physics - Condensed Matter* **16**, 7931-7939.
- Castaing, J., Girod, M., and Zink, A. (2004). Radiation background due to radioactivity in palaces and museums: influence on TL/ESR dating. *Journal of Cultural Heritage* **5**, 393-397.
- Chithambo, M. L. (2005). Towards models for analysis of time-resolved luminescence spectra from quartz. *Applied Radiation and Isotopes* **62**, 941-942.
- Chougaonkar, M. P., and Bhatt, B.C. (2004). Blue light stimulated luminescence in calcium fluoride, its characteristics and implications in radiation dosimetry. *Radiation Protection Dosimetry* **112**, 311-321.
- Correcher, V., Valle-Fuentes, F. J., and Garcia-Guinea, J. (2004). Radioluminescence and thermoluminescence emission spectra of a leucite of Monte Somma (Italy) (in Spanish). *Boletín de la Sociedad Española de Cerámica y Vidrio* **43**, 919-924.
- De Corte, F., Dejaeger, M., Hossain, S. M., Vandenberghe, D., De Wispelaere, A., and Van den Haute, P. (2005). A performance comparison of k(0)-based ENAA and NAA in the (K, Th, U) radiation dose rate assessment for the luminescence dating of sediments. *Journal of Radioanalytical and Nuclear Chemistry* **263**, 659-665.
- Deckers, K., Sanderson, D. C. W., and Spencer, J. Q. (2005). Thermoluminescence screening of non-diagnostic sherds from stream sediments to obtain a preliminary alluvial chronology: an example from Cyprus. *Geoarchaeology* **20**, 67-77.

- Dhir, R. P., Tandon, S. K., Sareen, B. K., Ramesh, R., Rao, T. K. G., Kailath, A. J., and Sharma, N. (2004). Calcretes in the Thar desert: genesis, chronology and palaeoenvironment. *Proceedings of the Indian Academy of Sciences- Earth and Planetary Sciences* **113**, 473-515.
- Duttine, M., Guibert, P., Perraut, A., Lahaye, C., Bechtel, F., and Villeneuve, G. (2005). Effects of thermal treatment on TL and EPR of flints and their importance in TL-dating: application to French Mousterian sites of Les Forets (Dordogne) and Jiboui (Drome). *Radiation Measurements* **39**, 375-385.
- Eitel, B., Hecht, S., Machtle, B., Schukraft, G., Kadereit, A., Wagner, G. A., Kromer, B., Unkel, I., and Reindel, M. (2005). Geoarchaeological evidence from desert loess in the Nazca-Palpa region, southern Peru: palaeoenvironmental changes and their impact on pre-Columbian cultures. *Archaeometry* **47**, 137-158.
- Engin, B. (2004). Use of thermoluminescence technique for the detection of irradiated spices. *Journal of Food Science and Technology - Mysore* **41**, 368-373.
- Ganzawa, Y., Furukawa, H., Hashimoto, T., Sanzelle, S., Miallier, D., and Pilleyre, T. (2005). Single grains dating of volcanic quartz from pyroclastic flows using red TL. *Radiation Measurements* **39**, 479-487.
- Gibling, M. R., Tandon, S. K., Sinha, R., and Jain, M. (2005). Discontinuity-bounded alluvial sequences of the southern Gangetic Plains, India: aggradation and degradation in response to monsoonal strength. *Journal of Sedimentary Research* **75**, 369-385.
- Gotze, J., Plotze, M., and Trautmann, T. (2005). Structure and luminescence characteristics of quartz from pegmatites. *American Mineralogist* **90**, 13-21.
- Hebenstreit, R., and Bose, M. (2003). Geomorphological evidence for Late Pleistocene glaciation in the high mountains of Taiwan dated with age estimates by optically stimulated luminescence (OSL). *Zeitschrift fur Geomorphologie* **47**, 31-49.
- Hetzel, R., Tao, M. X., Stokes, S., Niedermann, S., Ivy-Ochs, S., Gao, B., Strecker, M. R., and Kubik, P. W. (2004). Late Pleistocene/Holocene slip rate of the Zhangye thrust (Qilian Shan China) and implications for the active growth of the northeastern Tibetan Plateau. *Tectonics* **23**, TC6006.
- Koster, E. A. (2005). Recent advances in luminescence dating of late Pleistocene (cold-climate) aeolian sand and loess deposits in western Europe. *Permafrost and Periglacial Processes* **16**, 131-143.
- Lawless, J. L., Chen, R., Lo, D., and Pagonis, V. (2005). A model for non-monotonic dose dependence of thermoluminescence (TL). *Journal of Physics - Condensed Matter* **17**, 737-753.
- Lepczyk, X. C., and Arbogast, A. F. (2005). Geomorphic history of dunes at Petoskey State Park, Petoskey, Michigan. *Journal of Coastal Research* **21**, 231-241.
- Lu, H. Y., Wang, X. Y., Ma, H. Z., Tan, H. B., Vandenberghe, J., Miao, X. D., Li, Z., Sun, Y. B., An, Z. S., and Cao, G. C. (2004). The plateau monsoon variation during the past 130 kyr revealed by loess deposit at northeast Qinhai-Tibet (China). *Global and Planetary Change* **41**, 207-214.
- Madsen, A. T., Murray, A. S., Andersen, T. J., Pejrup, M., and Breuning-Madsen, H. (2005). Optically stimulated luminescence dating of young estuarine sediments: a comparison with Pb-210 and Cs-137 dating. *Marine Geology* **214**, 251-268.
- Marchioni, E., Horvatovich, N., Charon, H., and Kuntz, F. (2005). Detection of irradiated ingredients included in low quantity in non-irradiated food matrix. 2. ESR analysis of mechanically recovered poultry meat and TL analysis of spices. *Journal of Agricultural and Food Chemistry* **53**, 3774-3778.
- Mathew, G., Rao, T. K. G., Sohoni, P. S., and Karanth, R. V. (2004). ESR dating of interfault gypsum from Katrol hill range, Kachchh, Gujurat: implications for neotectonism. *Current Science* **87**, 1269-1274.

Mauz, B., and Felix-Henningsen, P. (2005). Palaeosols in Saharan and Sahelian dunes of Chad: archives of Holocene North African climate changes. *The Holocene* **15**, 453-458.

McIntosh, P. D., Kiernan, K., and Price, D. M. (2004). An aeolian sediment pulse at c.28 kyr BP in southern Tasmania. *Journal of the Royal Society of New Zealand* **34**, 369-379.

Miao, X. D., Mason, J. A., Goble, R. J., and Hanson, P. R. (2005). Loess record of dry climate and aeolian activity in the early- to mid-Holocene, central Great Plains, North America. *The Holocene* **15**, 339-346.

Otvos, E. G. (2005). Numerical chronology of Pleistocene coastal plain and valley development; extensive aggradation during glacial low sea-levels. *Quaternary International* **135**, 91-113.

Oviatt, C. G., Miller, D. M., McGeehin, J. P., Zachary, C., and Mahan, S. (2005). The Younger Dryas phase of Great Salt Lake, Utah, USA. *Palaeogeography, Palaeoclimatology, Palaeoecology* **219**, 263-284.

Personius, S. F., and Mahan, S. A. (2005). Unusually low rates of slip on the Santa Rosa range fault zone, northern Nevada. *Bulletin of the Seismological Society of America* **95**, 319-333.

Ponnusamy, V., and Ramasamy, V. (2004). Thermally stimulated luminescence sensitivity changes in biotite-granitic quartz as a result of annealing. *Indian Journal of Physics and Proceedings of the Indian Association for the Cultivation of Science* **78**, 1199-1203.

Poolton, N. R. J., Pantos, E., Hamilton, B., Denby, P. M., and Johnsen, O. (2004). Application of wavelength-resolved optically-detected XAS methods to phase-segregated silicates. *Physica Status Solidi B* **241**, 3656-3663.

Preusser, F., Radies, D., Driehorst, F., and Matter, A. (2005). Late Quaternary history of the coastal Wahiba Sands, Sultanate of Oman. *Journal of Quaternary Science* **20**, 395-405.

Rink, W. J., and Schwarcz, H. P. (2005). ESR and uranium series dating of teeth from the lower paleolithic site of Gesher Benot Ya'akov, Israel: confirmation of paleomagnetic age indications. *Geoarchaeology* **20**, 57-66.

Schellmann, G., Radtke, U., Scheffers, A., Whelan, F., and Kelletat, D. (2004). ESR dating of coral reef terraces on Curacao (Netherlands Antilles) with estimates of younger Pleistocene sea level elevations. *Journal of Coastal Research* **20**, 947-957.

Short, M. A. (2005). Polarization effects in the excitation and emission of Fe<sup>3+</sup> in orthoclase and their relevance to the determination of lattice sites of unknown defects. *Journal of Physics - Condensed Matter* **17**, 205-220.

Sivia, D. S., Burbidge, C., Roberts, R. G., and Bailey, R. M. (2004). A Bayesian approach to the evaluation of equivalent doses in sediment mixtures for luminescence dating. In "Bayesian Inference and Maximum Entropy Methods in Science and Engineering." (R. Fischer, R. Preuss, and U. v. Toussaint, Eds.), pp. 305-311. American Institute of Physics, Garching bei Munchen.

Skinner, A. R., Chasteen, N. D., Shao, J. L., Goodfriend, G. A., and Blackwell, B. A. B. (2005). Q-band ESR spectra as indicators of fossilization in tooth enamel. *Quaternary International* **135**, 13-20.

Srivastava, P., Brook, G. A., and Marais, E. (2004). A record of fluvial aggradation in the northern Namib Desert during the Late Quaternary. *Zeitschrift fur Geomorphologie, Supplement* **133**, 1-18.

Srivastava, P., Brook, G. A., and Marais, E. (2005). Depositional environment and luminescence chronology of the Hoarusib River Clay Castles sediments, northern Namib Desert, Namibia. *Catena* **59**, 187-204.

Sudan, P., Whitmore, G., Uken, R., and Woodbourn, S. (2004). Quaternary evolution of the coastal dunes between Lake Hlabane and Cape St Lucia, KwaZulu-Natal. *South African Journal of Geology* **107**, 355-376.

Sunta, C. M., Ayta, W. E. F., Chubaci, J. F. D., and Watanabe, S. (2005). A critical look at the kinetic models of thermoluminescence - II Non-first order kinetics. *Journal of Physics D* **38**, 95-102.

- Tatumi, S. H., Kinoshita, A., Fukumoto, M. E., Courriol, L. C., Kassab, L. R. P., Baffa, O., and Munita, C. S. (2005). Study of paramagnetic and luminescence centers of microcline feldspar. *Applied Radiation and Isotopes* **62**, 231-236.
- Thomas, P. J., Jain, M., Juyal, N., and Singhvi, A. K. (2005). Comparison of single-grain and small-aliquot OSL dose estimates in <3000 years of river sediments from South India. *Radiation Measurements* **39**, 457-469.
- Tomaz, L., Ferraz, G. M., and Watanabe, S. (2005). EPR and TL studies of phenakite crystal and application to dating. *Nuclear Instruments and Methods in Physics Research B* **229**, 253-260.
- Toyoda, S., Takeuchi, T., Aai, T., Komuro, K., and Horikawa, Y. (2005). Spin-spin relaxation times of the E1' center in quartz with and without irradiation: implications for the formation process of the oxygen vacancies in nature. *Radiation Measurements* **39**, 503-508.
- Trukhin, A., Liblik, P., Lushchik, C., and Jansons, J. (2004). UV cathodoluminescence of crystalline alpha-quartz at low temperatures. *Journal of Luminescence* **109**, 103-109.
- Turkin, A. A., van Es, H. J., Vainshtein, D. I., and den Hartog, H. W. (2005). Simulation of the effects of the dose rate and temperature on zircon thermoluminescence. *Journal of Physics D* **38**, 156-171.
- Wallinga, J., Tornqvist, T. E., Busschers, F. S., and Weerts, H. J. T. (2004). Allogenic forcing of the late Quaternary Rhine-Meuse fluvial record: the interplay of sea-level change, climate change and crustal movements. *Basin Research* **16**, 535-547.
- Yang, X.-Y., Kadereit, A., Wagner, G. A., Wagner, I., and Zhang, J.-Z. (2005). TL and IRSL dating of Jiahu relics and sediments: clue of 7th millennium BC civilization in central China. *Journal of Archaeological Science* **32**, 1045-1051.
- Yang, Y. X., Wu, X. M., Lin, J., Liu, Q. C., Den, J. Z., Huang, H. B., Jiang, Z. Y., and Hsia, Y. F. (2004). Soil thermoluminescence at Xi-wang deposit, Xiazhuang uranium ore field, China. *Journal of Radioanalytical and Nuclear Chemistry* **262**, 673-678.
- Zazo, C., Mercier, N., et al. (2005). Landscape evolution and geodynamic controls in the Gulf of Cadiz (Huelva coast, SW Spain) during the Late Quaternary. *Geomorphology* **68**, 269-290.

**Selected papers from the Proceedings of the 6th International Symposium on ESR Dosimetry and Applications that was held in Brazil in 2003. Publication was in Issue 2 of Volume 62 of Applied Radiation and Isotopes**

Bhat, M. (2005). EPR tooth dosimetry as a tool for validation of retrospective doses: an end-user perspective. *Applied Radiation and Isotopes* **62**, 155-161.

Blackwell, B. A. B., Liang, S. S., Golovanova, L. V., Doronichev, V. B., Skinner, A. R. and Blickstein, J. I. B. (2005). ESR at Treugol'naya Cave, Northern Caucasus Mt., Russia: Dating Russia's oldest archaeological site and paleoclimatic change in Oxygen Isotope Stage 11. *Applied Radiation and Isotopes* **62**, 237-245.

Chen, F., Graeff, C. F. O. and Baffa, O. (2005). K-band EPR dosimetry: small-field beam profile determination with miniature alanine dosimeter. *Applied Radiation and Isotopes* **62**, 267-271.

Chumak, V. V., Sholom, S. V., Bakhanova, E. V., Pasalskaya, L. F. and Musijachenko, A. V. (2005). High precision EPR dosimetry as a reference tool for validation of other techniques. *Applied Radiation and Isotopes* **62**, 141-146.

El-Faramawy, N. A. (2005). Comparison of gamma- and UV-light-induced EPR spectra of enamel from deciduous molar teeth. *Applied Radiation and Isotopes* **62**, 191-195.

El-Faramawy, N. A. (2005). Estimation of radiation levels by EPR measurement of tooth enamel in Indian populations. *Applied Radiation and Isotopes* **62**, 207-211.

El-Mabhouth, A. and Mercer, J. R. (2005). Re-188-labeled bisphosphonates as potential bifunctional agents for therapy in patients with bone metastases. *Applied Radiation and Isotopes* **62**, 541-549.

Ertay, T., Unak, P., Tasci, C., Zihnioglu, F. and Durak, H. (2005). Scintigraphic imaging with Tc-99m exorphin C in rabbits. *Applied Radiation and Isotopes* **62**, 883-888.

Gehrke, R. J. and Davidson, J. R. (2005). Acquisition of quality gamma-ray spectra with HPGe spectrometers. *Applied Radiation and Isotopes* **62**, 479-499.

Hassan, G. M. and Sharaf, M. A. (2005). ESR dosimetric properties of some biomineral materials. *Applied Radiation and Isotopes* **62**, 375-381.

Iwasaki, A., Grinberg, O., Walczak, T. and Swartz, H. M. (2005). In vivo measurements of EPR signals in whole human teeth. *Applied Radiation and Isotopes* **62**, 187-190.

Iwasaki, A., Walczak, T., Grinberg, O. and Swartz, H. M. (2005). Differentiation of the observed low frequency (1200 MHz) EPR signals in whole human teeth. *Applied Radiation and Isotopes* **62**, 133-139.

Khan, R. F. H., Pekar, J., Rink, W. J. and Boreham, D. R. (2005). Retrospective radiation dosimetry using electron paramagnetic resonance in canine dental enamel. *Applied Radiation and Isotopes* **62**, 173-179.

Kinoshita, A., Franca, A. M., de Almeida, J. A. C., Figueiredo, A. M., Nicolucci, P., Graeff, C. O. and Baffa, O. (2005). ESR dating at K and X band of northeastern Brazilian megafauna. *Applied Radiation and Isotopes* **62**, 225-229.

Kinoshita, A., Karmann, I., da Cruz, F. W., Graeff, C. F. O. and Baffa, O. (2005). K-band ESR spectra of calcite stalagmites from southeast and south Brazil. *Applied Radiation and Isotopes* **62**, 247-250.

Matsuda, T., Yamanaka, C. and Ikeya, M. (2005). ESR study of Gd<sup>3+</sup> and Mn<sup>2+</sup> ions sorbed on hydroxyapatite. *Applied Radiation and Isotopes* **62**, 353-357.

Mittani, J. C. R., Cano, N. F. and Watanabe, S. (2005). Use of Pb-Pb (3+) center of the amazonite for dating. *Applied Radiation and Isotopes* **62**, 251-254.

- Regulla, D. F. (2005). ESR spectrometry: a future-oriented tool for dosimetry and dating. *Applied Radiation and Isotopes* **62**, 117-127.
- Santos, A. B., Rossi, A. M. and Baffa, O. (2005). Study of dental enamel and synthetic hydroxyapatite irradiated by EPR at K-band. *Applied Radiation and Isotopes* **62**, 213-217.
- Sato, H. and Ikeya, M. (2005). Possibility of precipitated CaCO<sub>3</sub> with vitamin C as a new dosimetric material. *Applied Radiation and Isotopes* **62**, 337-341.
- Sholom, S. V. and Chumak, V. V. (2005). Variability of parameters in retrospective EPR dosimetry with teeth for Ukrainian population. *Applied Radiation and Isotopes* **62**, 201-206.
- Skinner, A. R., Blackwell, B. A. B., Martin, S., Ortega, A., Blickstein, J. I. B., Golovanov, L. V. and Doronichev, V. B. (2005). ESR dating at Mezmaiskaya Cave, Russia. *Applied Radiation and Isotopes* **62**, 219-224.
- Takeya, K., Tani, A., Yada, T. and Ikeya, M. (2005). ESR investigation of gamma-irradiated natural methane hydrate from Blake Ridge diapir, off east north America in ODP leg 164. *Applied Radiation and Isotopes* **62**, 371-374.
- Tani, A., Ueno, T., Yamanaka, C., Katsura, M. and Ikeya, M. (2005). Construction of imaging system for wide-field-range ESR spectra using localized microwave field and its case study of crystal orientation in suspension of copper sulfate pentahydrate (CuSO<sub>4</sub> center dot 5H<sub>2</sub>O). *Applied Radiation and Isotopes* **62**, 343-348.
- Tatumi, S. H., Kinoshita, A., Fukumoto, M. E., Courriol, L. C., Kassab, L. R. P., Baffa, O. and Munita, C. S. (2005). Study of paramagnetic and luminescence centers of microcline feldspar. *Applied Radiation and Isotopes* **62**, 231-236.
- Teixeira, M. I., Ferraz, G. M. and Caldas, L. V. E. (2005). EPR dosimetry using commercial glasses for high gamma doses. *Applied Radiation and Isotopes* **62**, 365-370.
- Teixeira, M. I., Ferraz, G. M. and Caldas, L. V. E. (2005). Sand for high-dose dosimetry using the EPR technique. *Applied Radiation and Isotopes* **62**, 359-363.
- Toyoda, S. (2005). Formation and decay of the E-1(′) center and its precursor in natural quartz: basics and applications. *Applied Radiation and Isotopes* **62**, 325-330.
- Toyoda, S., Tielewuhun, E., Romanyukha, A., Ivannikov, A., Miyazawa, C., Hoshi, M. and Imata, H. (2005). Comparison of three methods of numerical procedures for ESR dosimetry of human tooth enamel. *Applied Radiation and Isotopes* **62**, 181-185.
- Wieser, A., Debuyst, R., Fattibene, P., Meghziene, A., Onori, S., Bayankin, S. N., Blackwell, B., Brik, A., Bugay, A., Chumak, V., Ciesielski, B., Hoshi, M., Imata, H., Ivannikov, A., Ivanov, D., Junczewska, M., Miyazawa, C., Pass, B., Penkowski, M., Pivovarov, S., Romanyukha, A., Romanyukha, L., Schauer, D., Scherbina, O., Schultka, K., Shames, A., Sholom, S., Skinner, A., Skvortsov, V., Stepanenko, V., Tielewuhun, E., Toyoda, S. and Trompier, F. (2005). The 3rd international intercomparison on EPR tooth dosimetry: Part 1, general analysis. *Applied Radiation and Isotopes* **62**, 163-171.